PARAMETER MEASUREMENT OF 0.33 HP SYNCHRONOUS MACHINE USING ITECH DIGITAL POWER SUPPLY

A Thesis

presented to

the Faculty of California Polytechnic State University,

San Luis Obispo

In Partial Fulfillment

of the Requirements for the Degree

Master of Science in Electrical Engineering

by

Andrew Kargol

June 2023

COMMITTEE MEMBERSHIP

TITLE: Parameter Measurement of 0.33 HP Synchronous Machine Using ITECH Digital Power Supply

AUTHOR: Andrew Kargol

DATE SUBMITTED: June 2023

COMMITTEE CHAIR: Majid Poshtan, Ph.D.
Professor of Electrical Engineering

COMMITTEE MEMBER: Ali Shaban, Ph.D.
Professor of Electrical Engineering

COMMITTEE MEMBER: Ali Dehghan Banadaki, Ph.D.
Professor of Electrical Engineering

ABSTRACT

Parameter Measurement of 0.33 HP Synchronous Machine Using ITECH Digital Power Supply

Andrew Kargol

The classical methodologies for synchronous machine modeling provide a solid estimation for synchronous machine behavior but are limited in terms of accuracy due to the assumptions made in the modeling process. The equivalent circuit model developed by the classical approach breaks down the entire machine into a singular impedance component. This allows the model to be generated more quickly but limits its accuracy. In the pursuit of developing a more realistic model, this thesis outlines the parameter measurement of a Hampden SM-100 synchronous machine. In determining the SM-100's experimental parameters, this thesis executes and analyzes new experimental approaches to synchronous machine modeling. With the results of these approaches, a model for the Hampden SM-100 synchronous machine is developed that considers the rotor, stator, and core parameters of the synchronous machine separately.

Keywords: Synchronous Motor, Synchronous Generator, Electric Machines

ACKNOWLEDGMENTS

I would like to express my most sincere gratitude to Dr. Majid Poshtan. Dr. Poshtan provided unwavering support throughout the duration of my thesis and worked tirelessly to ensure this project was a success. I could not have asked for a better advisor, and I have been blessed to have had the opportunity to be under his mentorship.

I would also like to express my appreciation to my thesis committee members: Dr. Ali Dehghan Banadaki and Dr. Ali Shaban. Their efforts as my professors provided me with the necessary background to conduct this research and their knowledge and support as members of my thesis committee were critical to ensure my thesis was accurate, informative, and comprehensive.

Finally, I want to express my sincere gratitude to my family and friends for their continuous support in my undergraduate and graduate education. Their support has been critical to my academic success at Cal Poly.

TABLE OF CONTENTS

Page

LIST OF TABLES

Table Page

LIST OF FIGURES

Figure Page

1. INTRODUCTION

1.1 Synchronous Machine Overview

A synchronous electric machine is an alternating current (AC) electric machine with a rotor rotational speed that matches the speed of the stator's rotating magnetic field. There are two main components in synchronous machines, the stator, which remains stationary, and the rotor, the rotating component. The stator of a synchronous machine contains coils of wire known as windings in which three-phase AC current flows to create a rotating magnetic field inside the machine by Oersted's law. These windings are distributed evenly by phase around an iron core. The number of distinct windings in the stator will directly determine the operating speed of the motor. For each trio of three phase windings in the stator, a pair of poles is introduced. Using equation 1 with the number of stator pole pairs and the known electrical frequency, the steady state rotational speed can be calculated in rotations per minute (RPM). The rotor contains a constant magnetic field that is induced by an excitation circuit. This magnetic field interacts with the magnetic field of the stator to generate the force and rotation seen by a synchronous machine.

$$n_{sync}(RPM) = \frac{120 \times Frequency\ (Hz)}{Number\ of\ Poles} \tag{1}$$

Synchronous machines can act as either a motor or a generator depending on how the machine is configured. When the machine is functioning as a motor, the stator windings will receive a three-phase AC current input to generate a rotating magnetic field. The rotor poles generated by the excitation circuit follow the rotating magnetic field established by the stator to create rotor rotation and complete the conversion of electrical power to mechanical power. When the machine acts as a generator, the excitation circuit is energized, and the rotor is turned by a prime mover which creates a rotating magnetic field in the machine. This rotating magnetic field induces three-phase voltage on the stator windings by Faraday's Law and completes the conversion of mechanical power to electric power.

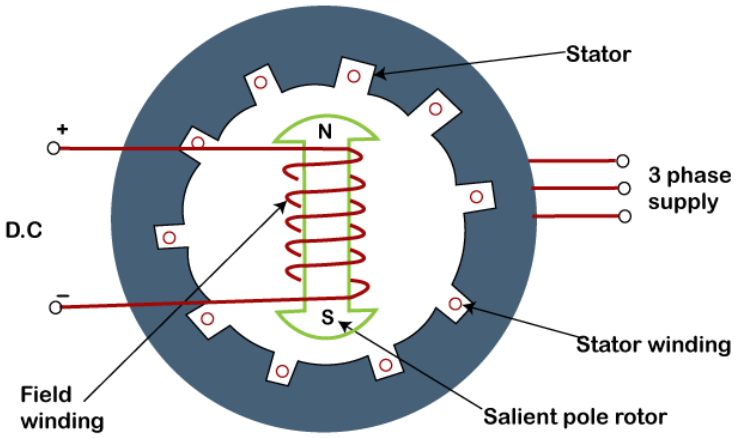

Figure 1: Synchronous Machine Component Diagram [1]

Synchronous generators are commonly used in utility scale generation applications. These generators produce power in a range of hundreds to thousands of MVA and establish the frequency of the electric grid. Synchronous motors are typically utilized in applications that require a constant speed. The level of DC excitation current in the rotor field windings of a synchronous machine can be used to set its power factor. A power factor of 1 is possible but can only be achieved if the DC excitation current supplied to the motor is the exact amount of excitation required for rotation. A high DC excitation current will result in a leading power factor as the stator magnetic field must oppose the rotor magnetic field. Conversely, a lower DC excitation current will result in a lagging power factor as the stator magnetic field must assist the rotor magnetic field to provide the required excitation for rotation.

2. CLASSICAL SYNCHRONOUS MACHINE MODELING

2.1 Electric Machine Non-Ideality

In an ideal electric machine, the input power given to the machine would be equal to the output power from the machine. Unfortunately, with physical machines there are many factors that influence the machine and reduce the system's output power. These factors can be split into three main categories: mechanical losses, copper losses, and core losses.

The mechanical losses of an electric machine are the losses an electric machine experiences due to forces impacting the physical rotation of the electric machine such as friction and windage. Friction losses of an electric machine exist in locations where opposition to the rotation of the rotor occurs. These losses are most prevalent in the bearings and brushes of electric machines where the opposition to rotation creates power loss through the generation of heat. The windage losses are losses due to the force required to overcome the air resistance that opposes rotor rotation.

Copper losses are losses due to current flow in the stator and rotor windings. These losses can be calculated by using equation 2, the current, and the resistance of the material in question. Copper losses are heavily impacted by increases in current as they are directly proportional to the square of the current.

$$P_{copper\ loss} = {I_{RMS}}^2 * R \tag{2}$$

The core losses of electric machines are losses that occur due to the presence of a changing magnetic field that can be categorized into eddy current and hysteresis loss. As the rotor rotates, it experiences a changing magnetic field from the AC stator windings. By Faraday's law this changing magnetic field induces a voltage on the rotor core. This core acts as a conductor for current flow which results in loss. To minimize this loss, the rotor of electric machines can be made up of thin laminations to increase the resistance of the core [2]. As the stator coils generate a changing magnetic field in the machine, the rotor core is magnetized and

demagnetized in each cycle. This process of magnetizing and demagnetizing the core in each cycle causes energy loss. This energy loss is due to hysteresis, which describes a material's ability to retain its polarization even as the current that induced that magnetism is set to zero. The total amount of power lost depends on various factors such as the operating frequency, voltage, current, and the material of the core. These factors can be identified and used with the BH curve of the material to calculate the total loss.

A BH curve shows the relationship between the magnetic flux density, B, and magnetic field intensity, H, for a given material and frequency. For a direct current operation, the hysteresis curve for a specific magnetic flux density can be used to directly find the magnetic field intensity. For the alternating current operation that is present in a synchronous machine, the BH curve is used in a different manner. As the current increases and decreases in each cycle, the magnetic field intensity increases and decreases with it. This causes the current to repeatedly trace a BH trajectory known as the hysteresis loop. The area enclosed within the hysteresis loop is equal to the hysteresis loss of the material in each cycle [3].

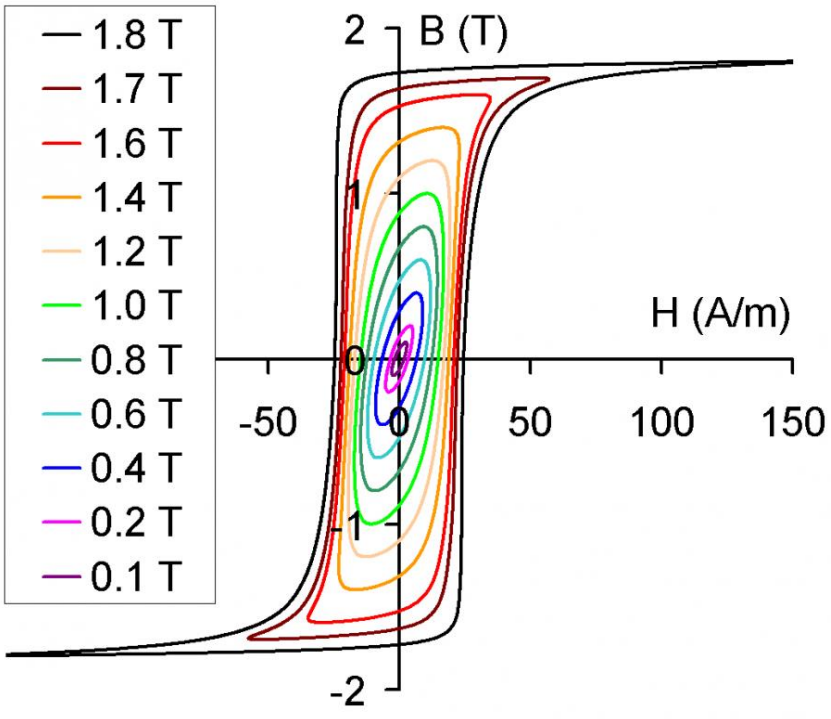

Figure 2: Example BH Curve with Hysteresis Loops

As the current and magnetic field intensity that the core of a synchronous machine experiences increases, the machine's point of operation moves vertically up the BH curve towards the point at which B, the magnetic flux density, no longer increases linearly. This point is known as saturation and represents the point at which a material is fully magnetized. For further increases to the magnetic flux intensity that the core experiences, the core's permittivity is reduced to the permittivity of a perfect vacuum. While the effect of saturation does harm the efficiency of the machine, it can assist the machine in responding to a significant change in load. If the machine is operating in the saturation region and a change in load moves the machine's operating position to a different point in the saturation region, the machine will experience a minimal change in flux density as the machine's permittivity is very low.

2.2 Synchronous Machine Circuit Modeling

To be able to predict and describe synchronous machine behavior, an electric circuit model can be used. There are different models that can be used, and each model has its own strengths and weaknesses. The selection of which model to use must be decided by factors such as the application of the machine, the degree of accuracy required for the model in question, and which parameters about the machine are known. The application of a synchronous machine will identify whether the machine is acting as a motor or generator. If the machine is acting as a generator, the induced voltage, commonly denoted E_a, will act as a source and current will flow from the induced voltage to the terminal voltage, commonly denoted V_t. Conversely, if the machine is acting as a motor, the terminal voltage will act as the source and current will flow from the voltage terminals to the induced voltage.

A complete equivalent circuit model for a three-phase synchronous machine can be seen in Figure 3. This complete model shows the rotor field circuit and all three phase windings to fully encapsulate the system. While this model provides the most details, showing all three phases and the rotor field circuit, it can be seen as repetitive and unnecessary. To reduce the number of parameters in the model, the model is frequently reduced to the per-phase model shown in Figure 4. In the per-phase model, the stator reactance, stator resistance, induced voltage, and terminal voltage are assumed to be the same for each phase. The stator resistance, denoted R_s, is the resistance of the stator coils and can be measured by applying a DC voltage across the stator terminal and using ohm's law to calculate the resistance. The synchronous reactance, X_s, represents the reactance due to a combination of the leakage and armature reactance. The effective impedance considering both X_s and R_s is known as the synchronous impedance and is denotated Z_S. The synchronous impedance can be found using equation 3 and the results of open and short circuit tests on a synchronous motor. Using the calculated Z_s and measured R_S, the synchronous reactance can be calculated using equation 4.

$$Z_s = \frac{E_F}{I_{SC}} = \frac{Open\ Circuit\ Per\ Phase\ Voltage}{Armature\ Short\ Circuit\ Current} \tag{3}$$

$$X_s = \sqrt{Z_s^2 - R_s^2} \tag{4}$$

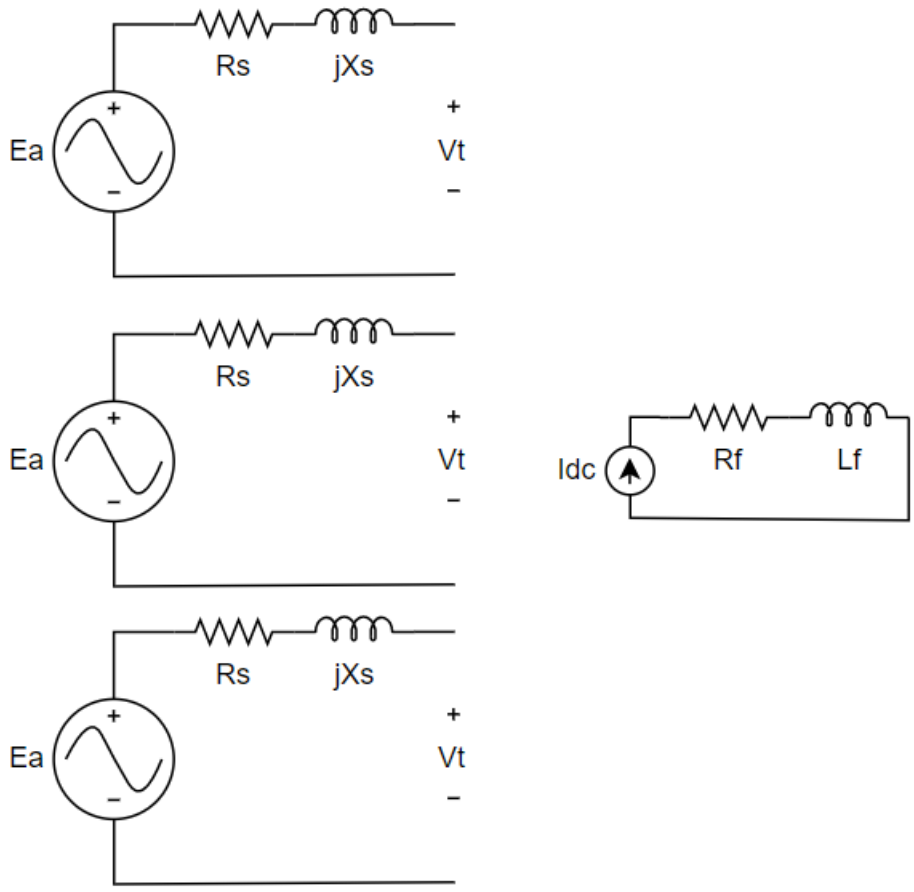

Figure 3: Three-Phase Synchronous Machine Equivalent Circuit Model

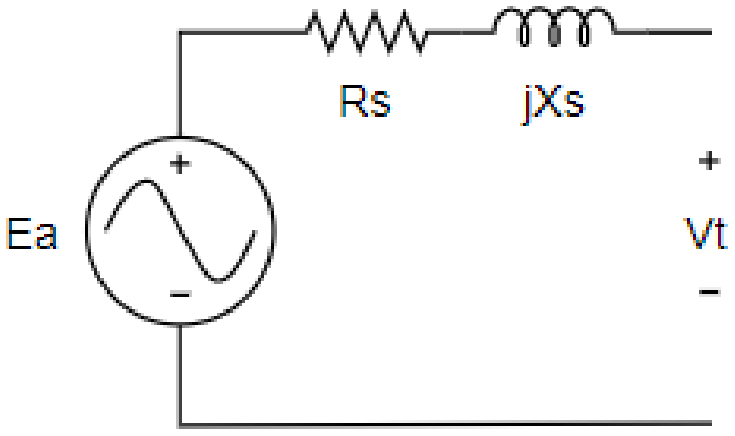

Figure 4: Per-Phase Synchronous Machine Equivalent Circuit Model

Using the parameters defined in this model, the output torque and power can be calculated for various operating conditions. The only additional parameter that must be considered is the torque angle, δ, the angle between the stator and rotor magnetic fields. The synchronous speed, ω_{sync}, of the machine in radians per second can be calculated through equation 5. If the armature resistance is ignored, the three-phase power and torque of the machines can be calculated using equation 6 and equation 7 respectively.

$$\omega_{sync} = \frac{n_{sync} \times 2\pi}{60} \tag{5}$$

$$P_{3Phase} = \frac{3 \times |V_t| \times |E_a|}{X_s} \sin\delta \tag{6}$$

$$T = \frac{3 \times |V_t| \times |E_a|}{\omega_{sync} \times X_s} \sin\delta \tag{7}$$

A more detailed model that separates the stator and core losses can be seen in Figure 5. This model was derived from the model for synchronous machines shown in reference 4, *Electric Machine Topologies in Energy Storage* Systems, with the rotor resistance and impedance being considered as part of the excitation circuit. The most significant change between this model and the basic model shown in Figure 4 is the addition of a core loss component. The core resistance R_C is placed in parallel with the induced voltage [4]. This allows for a more accurate model as the losses in the core and the stator can be separately modeled and more accurately tracked. Figure 5 was selected as the model to represent the parameters calculated in this thesis as a compromise between simplicity and accuracy.

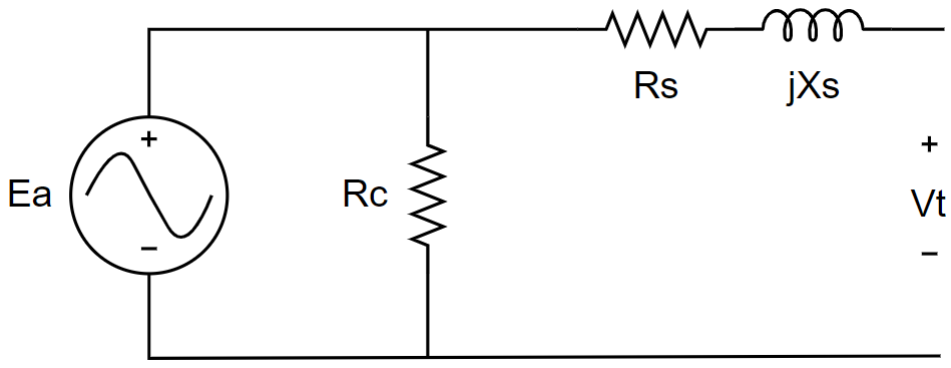

Figure 5: Per-Phase Synchronous Machine Equivalent Circuit Model with Core Loss [4]

3. OPERATION OF SYNCHRONOUS MACHINES

3.1 Synchronous Generator Operation

A synchronous generator can be grid-connected and operated with a link to the external power grid or can be isolated and disconnected from the external power grid. This section will outline the key differences between these two modes of operation.

3.1.1 Grid-Connected Synchronous Generator Operation

When a synchronous generator is grid connected, it becomes backed by the infinite bus that is present due to the large generators actively supporting the electric grid. With the inertia being provided by these large generators, the voltage magnitude, frequency, phase sequence, and phase angle of the synchronous generator must match the grid. The inertia of the grid works to ensure that the generator's voltage and frequency are unaffected by rapid changes in loading. If the excitation of the synchronous generator is increased in this state, the reactive power output of the generator increases. If the frequency of the prime mover is increased, the active power produced by the synchronous generator will increase.

3.1.2 Isolated Synchronous Generator Operation

An isolated synchronous generator is disconnected from the electric grid and thus is more vulnerable to changes in the system loading. Without the inertia that is present in the grid, the voltage magnitude, frequency, and phase angle are dependent on the generator operation. The frequency of the synchronous machine will be set based on the speed of the prime mover, the phase angle is dependent on the system loading, and the level of excitation current will directly impact the terminal voltage. An increase in the excitation current will result in an increase in the terminal voltage. Without the support of the grid, an overload on the generator could occur if the load placed on the generator is too high. This will result in a reduction of the speed of the rotor and a corresponding drop in the system frequency.

3.2 Synchronous Motor Operation

Synchronous motors are not self-starting and thus require an external methodology to bring the rotor to near synchronous speed. This section explains why an external starter is needed, explains the principle behind the induction start used in the experiments outlined in this thesis, and provides background information on induction machine modeling.

3.2.1 Synchronous Motor Start-Up

Synchronous motors are unable to start without an external stimulus. As seen in the torque speed characteristic curve for a synchronous motor in Figure 6, a synchronous motor is unable to generate torque at any speed other than its synchronous speed. This does not cause an issue for the rated operation of the machine but prevents the machine from starting as it is unable to produce torque when its rotor is not rotating. For this reason, many synchronous motors, including the SM-100 machine under test in this thesis, use an induction start to initiate the rotation of the rotor. The torque-speed characteristic of an induction motor shown in Figure 7, highlights that when the machine is not rotating, the induction machine is still able to produce a torque. This torque will allow the rotor's rotation to start and approach synchronous speed. When the induction-start has been completed and the rotor is near synchronous speed, the DC excitation current can be provided to the rotor. As soon as the excitation current is provided, the rotor and stator magnetic fields reach synchronism, and the machine begins operating at synchronous speed.

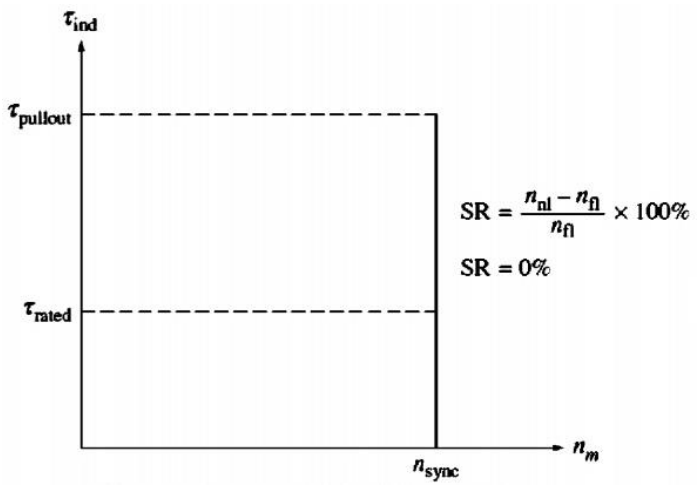

Figure 6: Torque-Speed Characteristic Curve of Synchronous Motor [5]

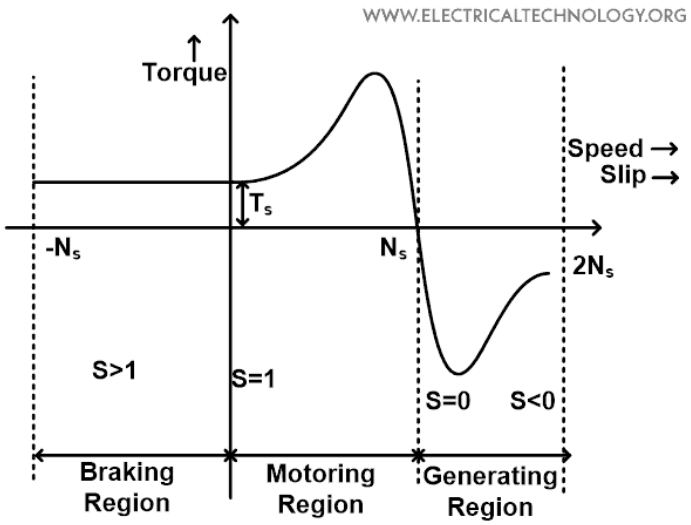

Figure 7: Torque-Speed Characteristic Curve of Induction Motor [6]

3.2.2 Squirrel Cage Induction Machine Overview

An induction machine is an AC electric machine with a rotational speed that varies with changes in the load placed upon it. As was described with synchronous machines, there are two main components in induction machines, the rotor and stator. The stator of a squirrel cage induction machine follows the same construction and operating principle of a synchronous machine to induce a magnetic field by Oersted's law. While the stator construction of the two machine types is similar, the rotor construction and operating principles are different. The rotor of a squirrel cage induction machine does not contain a permanent magnet or an excitation circuit, but instead is typically made up of conductive bars of aluminum or copper that are shorted on both ends by end rings. The end ring and conductive bars are collectively known as a squirrel cage. The squirrel cage is not able to create a magnetic field on its own and instead has a voltage induced upon it by the rotating magnetic fields of the stator in accordance with the relationship defined in Faraday's Law in equation 8. This induced voltage creates a current across the shorted squirrel cage bars, which in turn generates its own magnetic field. This magnetic field follows the stator magnetic field to create rotation but does so at a speed that is slower than the synchronous speed of the machine. The relationship between the synchronous speed and the asynchronous machine rotational speed is defined as slip and can be found in equation 9. As the load on the induction machine increases the asynchronous speed of the machine drops, distancing itself from the synchronous speed and increasing the slip.

$$E_{ind} = -N\frac{d\Phi}{dt} \tag{8}$$

$$Slip = \frac{N_{sync} - N_{async}}{N_{sync}} \tag{9}$$

3.2.3 Induction Machine Circuit Modeling

A commonly used model for induction machines can be seen in Figure 8. In this model, the stator resistance is denoted as R_s, while X_S denotes the stator leakage reactance. The magnetizing reactance is denoted as X_M and is placed in parallel with the core resistance, R_C. The rotor resistance reflected to the stator is denoted as R_r, and X_r denotes the rotor reactance reflected to the stator. The slip of the machine is denotated as s and has a direct impact on the prevalence of the rotor resistance in the circuit. As the slip decreases and the rotor approaches synchronous speed the rotor resistance approaches infinity. For the induction modeling to be completed in this report, the model shown in Figure 8 will be used.

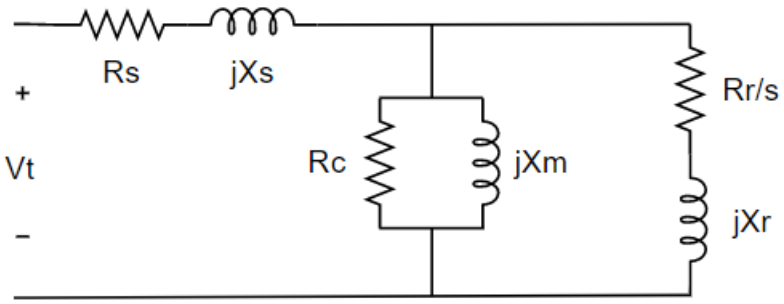

Figure 8: Per-Phase Induction Machine Equivalent Circuit Model

4. EXPERIMENTAL EQUIPMENT SPECIFICATIONS AND DESIGN

4.1 Experimental Specifications

In this thesis, experiments were conducted on Hampden SM-100 synchronous machines to define a comprehensive model for the SM-100. Table 1 outlines the specifications for the Hampden SM-100 synchronous machine and the additional equipment used in the synchronous machine experiments in this thesis. The SM-100 is shown in Figure 9 and Figure 10.

Table 1: Equipment Specifications

Equipment	Specifications
Hampden SM-100 Synchronous Machine	Manufacturer and Model: Hampden SM-100 AC Voltage: 208/120 V 3Φ-4W Rated DC Voltage: 125 Rated Speed: 1800 RPM Load Current Rating: 1.7 A Maximum Excitation Current Rating: 1.6 A Rated DC 1.2 A Rated Power: 250 W AC Frequency: 60 Hz
Dynamometer	Manufacturer and Model: Magtrol HD-705-6 Maximum Torque: 50 lb-in Maximum Speed: 25000 RPM
Resistive Load	Nominal Resistance: 35 Ω Rated Voltage: 125 V Maximum Current: 3.7 A
Inductive Load	Manufacturer and Model: Hammond 195P10 Inductance: 30 mH Maximum Current: 10 A
ITECH DC Power Supply	Manufacturer and Model: ITECH IT-M3633 Maximum Output Voltage: 150 V Maximum Output Current: 12 A Maximum Output Power: 800 W

Figure 9: Hampden SM-100 Front Panel

Figure 10: Hampden SM-100 Synchronous Machine

The Hampden SM-100 is a four pole 208/120 V 1/3 HP three-phase synchronous machine that can be operated as a synchronous motor or a synchronous generator. The machine's rotor contains a squirrel cage and an induction-start switch. When the switch is on induction-start, the field excitation circuit is short circuited. This allows the machine to start as an induction machine to reach its asynchronous speed with both the damper winding and field winding acting as a squirrel cage. After the induction start is completed, the switch can be flipped to synchronous run, thus removing the short circuit across the field winding. If a DC input is not applied to the DC excitation current terminal, the field winding will be open circuited. This will keep the machine running at asynchronous speed as the damper winding is always short circuited, but with less torque provided. If a DC input is provided and the synchronous run position is selected, the machine will have a closed excitation circuit and will run at synchronous speed. The associated schematics for SM-100's operation as a synchronous motor and synchronous generator can be found in Figure 11 and Figure 12 [7].

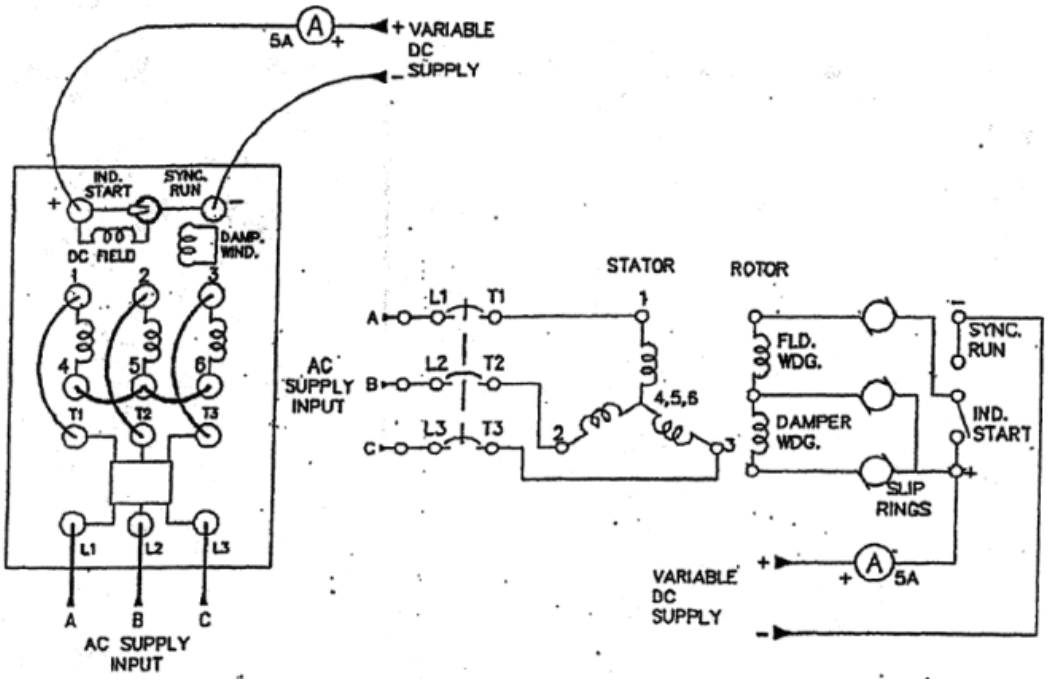

Figure 11: Hampden SM-100 Synchronous Motor Circuit Schematic [7]

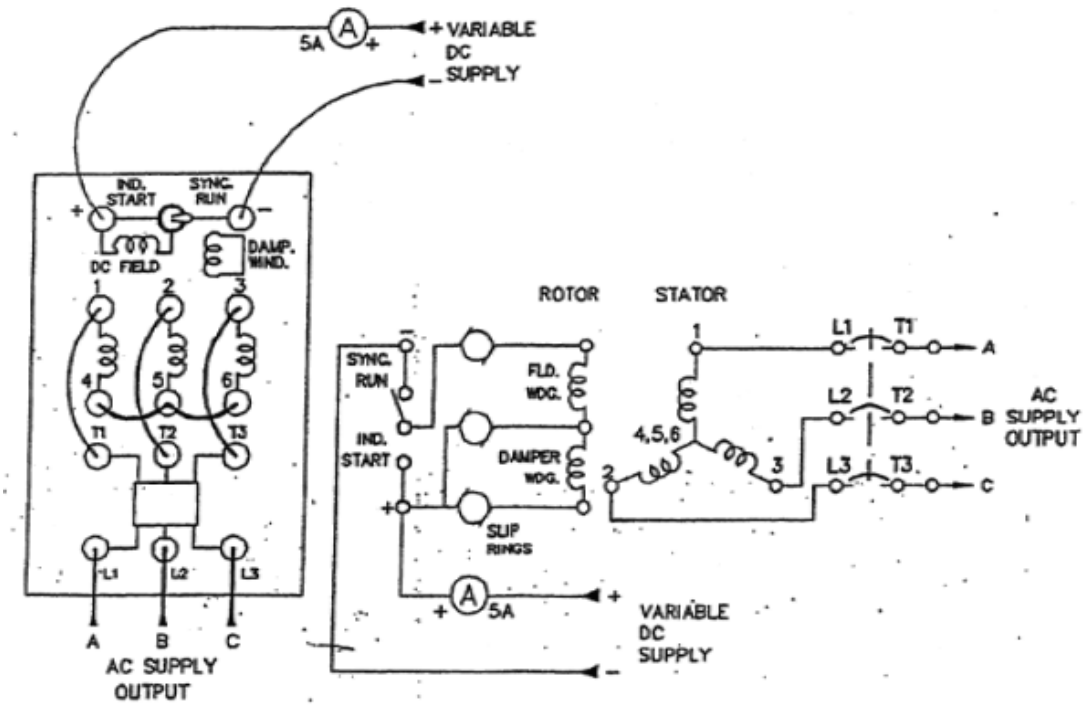

Figure 12: Hampden SM-100 Synchronous Generator Circuit Schematic [7]

For the experiments conducted in this thesis, the DC supply for the synchronous machine was provided by the ITECH IT-M3633 Regenerative Power System. The IT- M3633 was used as a source in a constant output current mode that automatically increases or decreases the DC input voltage to ensure a constant current is provided to the DC input terminals. The system can be fine-tuned to change the output current in increments as low as 1 mA and has extensive protection settings to protect the device itself and the load that is receiving its output. Further details regarding the operation and function of the IT-M3633 can be found through documentation on the ITECH website [8].

4.2 Experimental Configuration

In the experiments conducted in this thesis to develop a synchronous machine model, the SM-100 synchronous machines were used as synchronous generators, synchronous motors, and induction motors. When experiments were conducted on the SM-100 as a motor, it received its three-phase stator input power from the Cal Poly Energy Conversion Laboratory's 208/120V 60 Hz source. During the SM-100's testing as a generator, another SM-100 was used as its prime mover via a coupling at each machine's rotor as shown in Figure 13 and Figure 14.

Figure 13: Coupled Hampden SM-100 Front Panel View

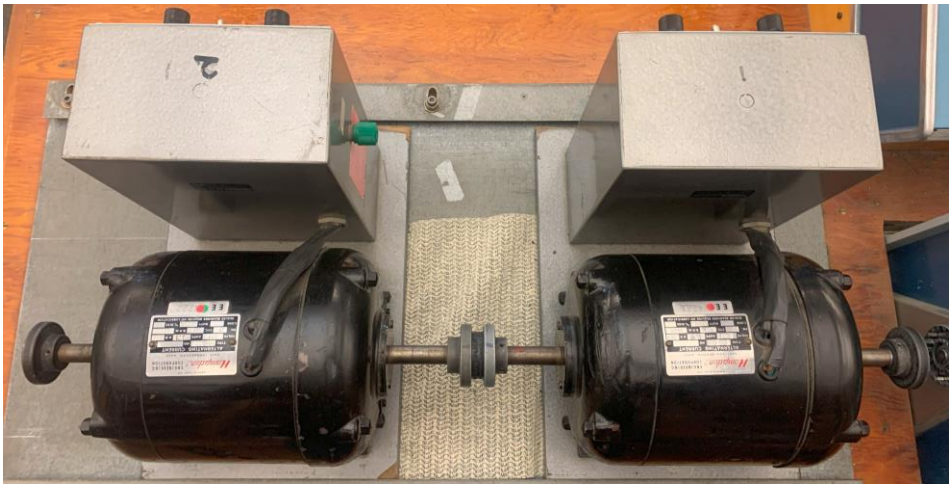

Figure 14: Coupled Hampden SM-100 Synchronous Machine View

5. SYNCHRONOUS MACHINE EXPERIMENTS

In this thesis, experiments were conducted to measure the equivalent circuit parameters, mutual inductance, and stator to rotor turns ratio of the Hampden SM-100 synchronous machine and observe how the machine responded to different test conditions. This section outlines how the experiments were conducted and analyzes the data that was collected from the experiments.

5.1 Synchronous Motor "V Curve" Experiment

One of the most common experiments for synchronous motors is the "V curve" experiment. This experiment was conducted to show the relationship between the stator armature current and the field current for the SM-100's operation as a motor. As can be seen in the plotted output data of Figure 17, the experiment's name comes from the shape of its curve when the armature current is plotted vs the field current. This experiment was conducted for a test condition with an unloaded torque of 0.33 lb-in and loaded condition of 7.01 lb-in to see how the relationship between armature current and field current changes with different loading conditions. The load torque was applied using the Magtrol HD-705-6 dynamometer. When the desired torque was applied, the excitation current was varied by changing the output from the ITECH DC power supply. The circuit used to conduct this experiment can be seen in Figure 15 where the load torque block represents the Magtrol dynamometer. The experimental setup can be seen in Figure 16 and the full results from this experiment can be found in Appendix A.

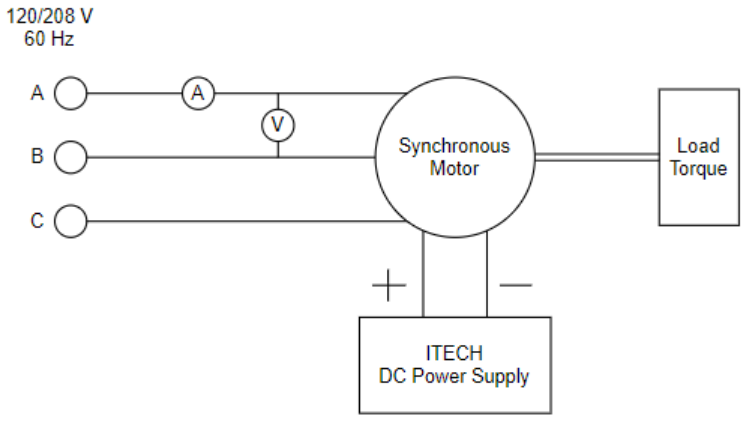

Figure 15: Synchronous Motor V Curve Experiment Schematic

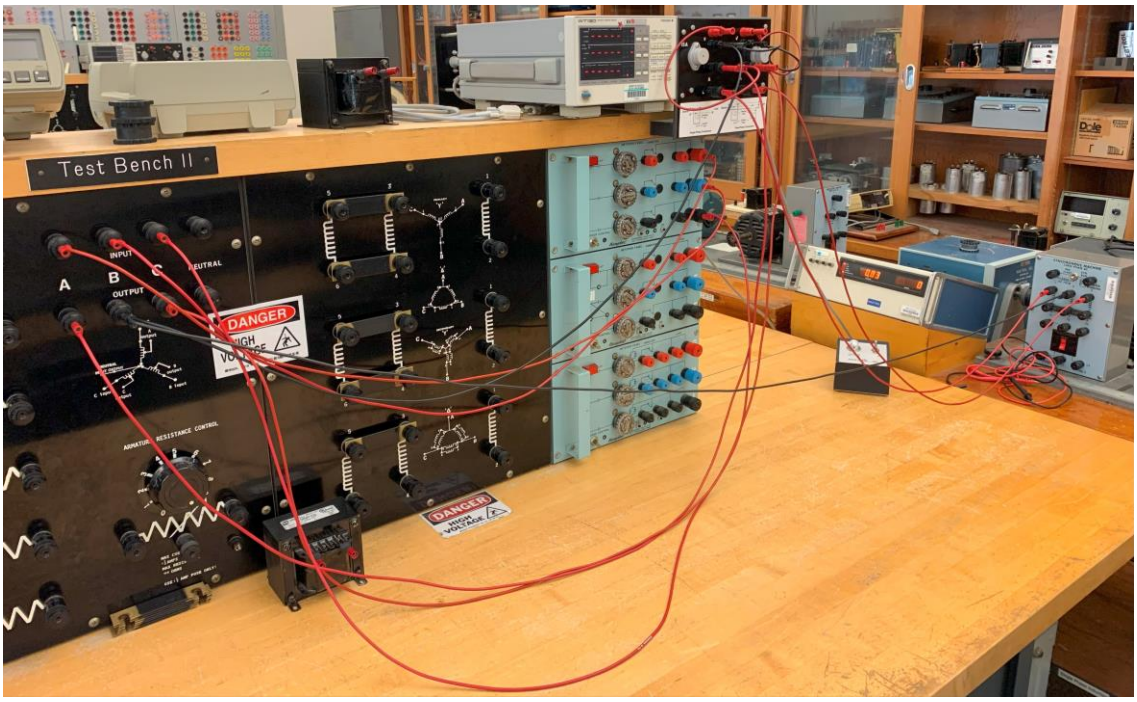

Figure 16: Synchronous Motor V Curve Experimental Setup

The most critical data points from the synchronous motor “V curve” experiment are highlighted in Figure 17 and Figure 18. The plots shown in Figure 17 are the “V curves” of the synchronous motor that express the relationship between the armature current and the field current. In comparing the unloaded and loaded plots in Figure 17, the machine requires more current to provide the additional load torque requirement for the loaded test. This additional stator current and the associated increase in excitation current move its V curve up and to the right of the no load curve. Figure 18 demonstrates that as the load increases the field current must increase with it to match the power factor of the unloaded motor case and improve the efficiency of the operation of the synchronous motor. In comparing Figure 17 and Figure 18, it can be seen that the field current data that corresponds to the lowest armature current value is the value at which the power factor is closest to 1. At this point almost all the power being supplied to the motor is real power, but as the field current of the machine is increased or decreased and the power factor decreases, reactive power becomes more prevalent. In the loaded curve, the maximum power factor occurs near a field current of 0.6 A. This result is as anticipated as 0.6 A is approximately half of $I_{DC\text{-}Rated}$ as calculated in equation 10 using the

measured resistance of the rotor. If the field current is less than the value at which the power factor is equal to 1, the power factor will be lagging, and the motor will be consuming reactive power from its source. Conversely, if the field current is greater than the value at which the power factor is equal to 1, the power factor will be leading, and the motor will be supplying reactive power back to its source. Figure 18 shows this relationship most directly as it plots the power factor vs the field current.

$$I_{DC-Rated} = \frac{V_{DC\ RATED}}{R_{rotor}} = \frac{125\ V}{102\Omega} \approx 1.225A \tag{10}$$

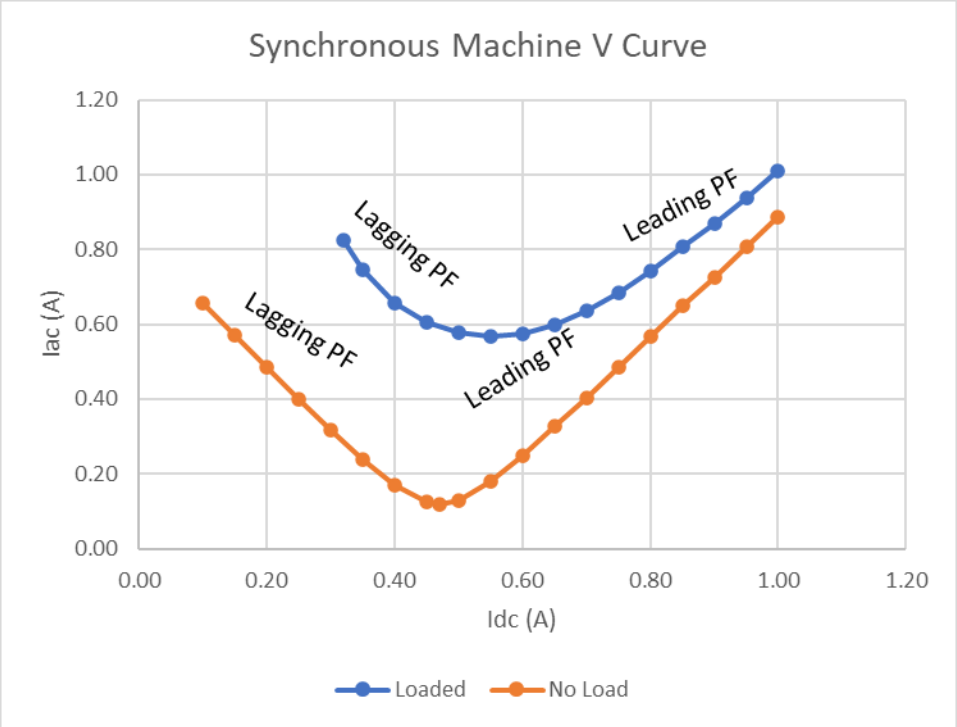

Figure 17: No Load and Loaded Synchronous Motor V Curves

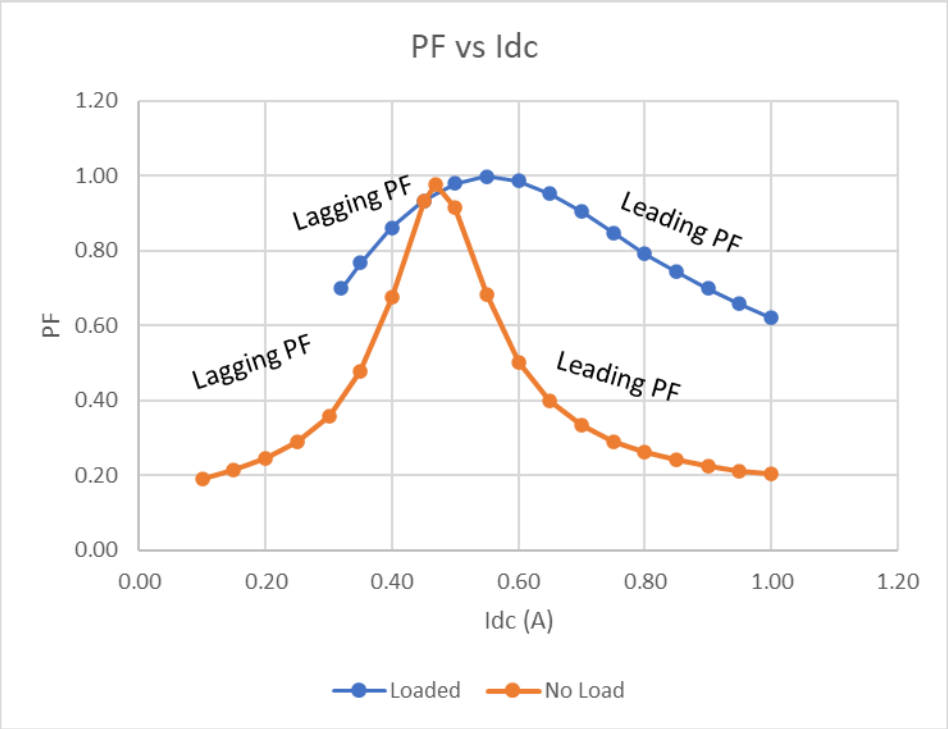

Figure 18: No Load and Loaded Power Factor vs Field Current

To measure the SM-100's ability to deliver power to a mechanical load as a motor, the output power was calculated and used to calculate the efficiency of the machine for the loaded test condition with 7.01 Lb-in of applied torque. Figure 19 shows the relationship between the efficiency and excitation current of the machine. As would be expected, the machine acts most efficiently in conditions where the input stator power factor is near 1. When the power factor is less than 1, the source is either consuming or sourcing reactive power. This increases the current through the stator coils which in turn increases the copper and core losses of the machine.

$$P_{mechanical-3Phase} = T_{load} * N_{sync} * 1.18 * 10^{-2} \quad (11)$$

$$Efficiency = \frac{P_{mechanical-3Phase}}{P_{input-3Phase}} \quad (12)$$

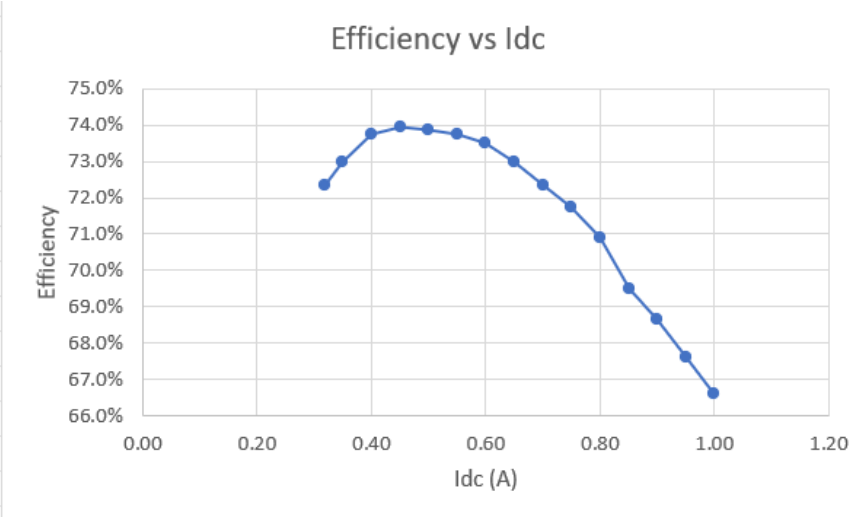

Figure 19: Efficiency vs I_{DC} Curve

In comparing the no-load and loaded cases with identical V_{in} and I_{DC}, the additional mechanical friction and loading is assumed to have no significant impact on the reactive power consumption of the motor. This is because the reactive power loss happens only across the stator series inductance and the iron magnetizing inductance. With this statement, it can be reasonably assumed that the reactive power produced in the iron should remain constant between the no-load and loaded cases. With this assumption the stator impedance of the synchronous machine can be calculated using the relationships expressed in equations 13-17 for an excitation current of 0.5 A. An excitation current of 0.5 A was selected for this calculation as both the unloaded and loaded test cases had a power factor that was near 1. This value provides a good estimation for the reactance of the stator, but a more accurate approach to model the stator reactance can be found in section 5.12, Temperature Effect on Coil Resistance and Stator Reactance.

$$\Delta Q = Q_{load} - Q_{no\ load} = 14\ VAR - 6.19\ VAR = 7.81\ VAR \tag{13}$$

$$Q_{total\ no\ load-1Phase} = I^2 * X_{stator} + Q_{iron} = 6.19\ VAR = (0.13)^2 X_{stator} + Q_{iron} \tag{14}$$

$$Q_{total\ loaded-1Phase} = I^2 * X_{stator} + Q_{iron} = 14\ VAR = (0.58)^2 X_{stator} + Q_{iron} \tag{15}$$

$$\Delta Q = 7.81\ VAR = 0.3195 * X_{stator} \tag{16}$$

$$X_{stator} = 24.45\Omega \tag{17}$$

The no load curve of the V curve experiment is a good approximation but does not provide a perfect model for a no-load condition. For the no-load condition completed in this test, a small load is placed on the machine from the internal friction of the dynamometer. This additional load causes error in the calculations completed in this section. To remedy this, a second no-load test was conducted with the motor decoupled from the dynamometer. This experiment is explained in the next section.

5.2 Synchronous Motor Mechanical Loss Experiments

Multiple experiments were conducted to determine the mechanical loss and an estimation for the core losses for the SM-100 at varying excitation currents. The first experiment conducted was a no-load synchronous motor test to determine the total power consumption for various DC excitation currents. The schematic for this experiment can be seen in Figure 20. In a second experiment, the same synchronous motor was coupled to a second synchronous machine to determine the extra mechanical loss required to rotate both machines. This second machine receives no input and is solely a mechanical load. The schematic for this experiment can be seen in Figure 21. The mechanical loss and core loss per machine can be estimated using the data calculated in these experiments and equations 18-20. The full results from this experiment can be found in Appendix B.

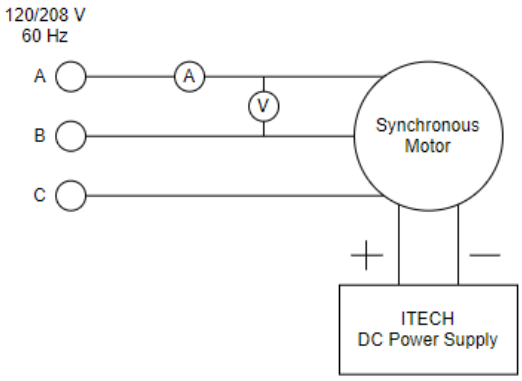

Figure 20: Synchronous Motor Mechanical Loss Test Uncoupled Case Schematic

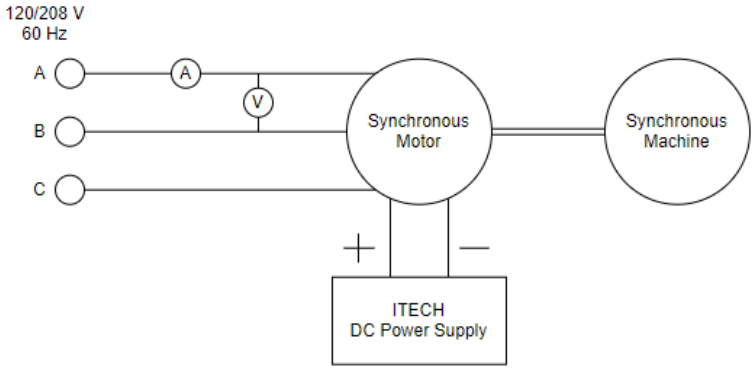

Figure 21: Synchronous Motor Mechanical Loss Test Coupled Case Schematic

To estimate the mechanical loss of the SM-100, the results of both experiments were compared. As both the machine under test and the machine acting as a mechanical load are the same model, the loss due to the mechanical load of the system is assumed to be doubled when the motor is run with the coupled synchronous machine. To calculate the per phase copper loss of the machine, a DC current was connected across one of the stator windings of the SM-100 and a resistance of 4.3Ω was calculated using ohm's law. With the stator resistance parameter identified, the per phase copper loss can now be calculated using equation 18. Using the calculated copper loss value, the mechanical and core loss for each test condition can be calculated with equation 19 and equation 20. The results of these calculations are summarized within Table 2.

$$\mathrm{P}_{\text{copper loss}-1\text{Phase}} = \mathrm{I}_{\mathrm{AC}}^{2} * R_{Stator} \tag{18}$$

$$\mathrm{P}_{\text{mechanical loss per machine}} = \mathrm{P}_{\text{coupled}} - \mathrm{P}_{\text{uncoupled}} - 3 * (\mathrm{P}_{\text{copper loss coupled}} - \mathrm{P}_{\text{copper loss uncoupled}}) \tag{19}$$

$$\mathrm{P}_{\text{core loss per machine}} = \mathrm{P}_{\text{measured}} - \mathrm{P}_{\text{mechanical loss per machine}} - \mathrm{P}_{\text{copper loss}} \tag{20}$$

Table 2: Mechanical Loss Test Power Loss Calculation

DC Excitation Current (A)	Mechanical Loss Per Machine (W)	Core Loss Per Machine (W)	Copper Loss (W)
0.4	20.84	6.37	0.111
0.5	19.94	9.00	0.034
0.6	20.45	10.08	0.202
0.7	21.42	10.96	0.609
0.8	22.04	12.80	1.254
0.9	23.97	13.49	2.113
1.0	26.07	13.91	3.173

The no-load test was conducted to set the baseline for the loaded mechanical test, but was also used to measure the impact of the internal friction of the dynamometer on the V-curve experiment. After the no-load test was completed, the power consumption was compared with

the results from the V-curve no load experiment. In the newly completed test, the lack of dynamometer caused the mechanical power loss to decrease. For example, for I_{DC} =0.5 A where PF is near 1, the difference in loss between the two tests was 6.32 W. All the results for this analysis can be seen in Table 3.

Table 3: No Load Dynamometer Loss Analysis

I_{DC} (A)	$P_{loss\ with\ dynamometer}$ (W)	$P_{loss\ without\ dynamometer}$ (W)	Difference in P_{loss} (W)
0.4	33.85	27.21	6.64
0.5	35.26	28.94	6.32
0.6	37.78	30.56	7.22
0.7	41.23	32.37	8.86
0.8	46.09	34.85	11.24
0.9	51.49	37.46	14.03
1	57.49	39.98	17.51

5.3 Preliminary Core Loss Parameter Measurement Experiment

The core losses of a machine can be a difficult parameter to calculate as there is no direct impedance to be measured as the losses occur due to hysteresis and eddy current. To calculate the core losses of the SM-100, the machine was set up as a synchronous motor and was placed under a full load test condition at a power factor of 1. With a power factor of 1, the reactive power consumed by the machine is eliminated and the machine operates with purely resistive losses. To achieve this condition, the experimental setup of Figure 22 was used with the synchronous motor connected to the Magtrol dynamometer. The full load torque to be applied to the machine was calculated to be 15.02 Lb-in using equations 21 and 22, the one-third horsepower rating of the machine, and the calculated $P_{mechanical\ loss}$ from the mechanical loss test that was closest to the required I_{DC} value. In this case, the required I_{DC} value was 0.778 A so the mechanical loss calculation for an I_{DC} of 0.8 A was used to approximate the amount of loss. The output data collected from this experiment is summarized in Table 4.

$$\mathrm{P_{mechanical}} = \frac{1}{3} * 1\ \mathrm{hp} = 248.67\ \mathrm{W} = \mathrm{Torque\ (Lb-in)} * \mathrm{n(RPM)} * \frac{1.18}{100} + \mathrm{P_{mech\ loss\ calculated}} \quad (21)$$

$$\mathrm{Torque\ (Lb-in)\ Applied} = (248.67 - 19.42) * \frac{118}{1800} = 15.02\ \mathrm{Lb-in} \quad (22)$$

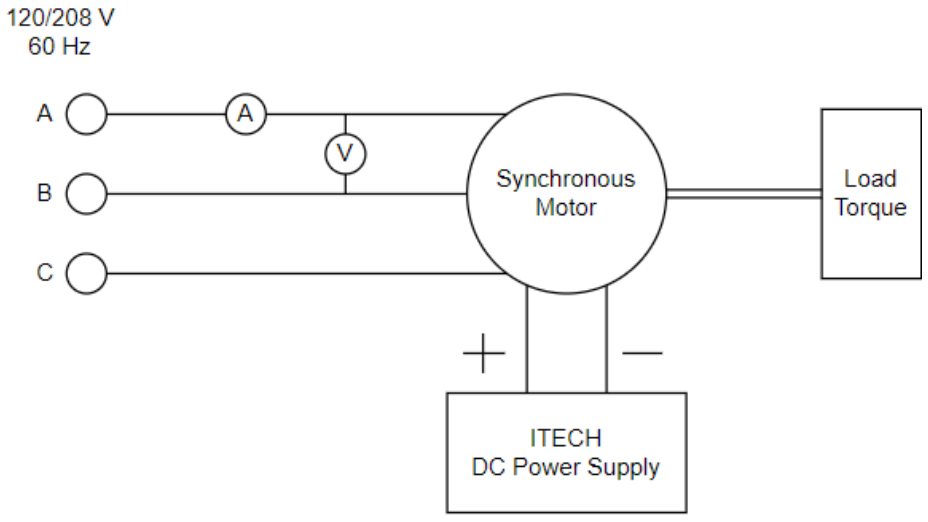

Figure 22: Schematic for Preliminary Core Loss Parameter Measurement

Using the collected data from this experiment, the core loss and an approximate core resistance parameter can now be calculated. With equation 23 the net mechanical power can be calculated using the torque and speed of the motor and the calculated mechanical loss for the I_{DC} of 0.8A. This value and the copper loss of the machine can be subtracted from the net input power measured to calculate a core loss of 54.11W. If the armature voltage loss is ignored, the core loss can be assumed to be directly proportional to the square of the terminal voltage. This assumption allows for an estimated core resistance parameter to be calculated to be 807.2 Ω using equation 25. This value of resistance does not physically exist within the machine, but instead is a representation of the hysteresis and eddy current losses at the full load condition.

$$\mathrm{P}_{\text{mechanical 3 Phase}} = \mathrm{T} * n(RPM) * \frac{1.18}{100} + \mathrm{P}_{\text{mechanical loss } \mathrm{I_{DC}}=0.8A} = 229.12 + 19.42 = 248.54 \quad (23)$$

$$\mathrm{P}_{\text{core loss per machine}} = \mathrm{P}_{3-\text{Phase}} - P_{mechanical\ 3\ Phase} - 3 * 4.3 * \mathrm{I}_{\mathrm{A}}^{2} = 54.11\ W \quad (24)$$

$$\mathrm{R}_{\mathrm{C-calc}} = \frac{{\mathrm{V_{LL}}}^{2}}{\mathrm{P}_{\text{core loss}}} = 807.2\ \Omega \quad (25)$$

Table 4: Preliminary Core Loss Parameter Measurement Calculation

I_{DC} (A)	V_{LL} (V)	I_a (A)	$P_{3\text{-Phase}}$ (W)	$S_{3\text{-Phase}}$ (VA)	PF	Torque (Lb-in)	Speed (RPM)	$R_{C\text{-calc}}$ (Ω)
0.778	209	1.129	409	409	1	15.02	1800	807.2

5.4 Rotor Windings Measurement Experiment

The rotor of the SM-100 consists of two windings, the field and damper windings. The damper winding is present in the SM-100 in the form of a squirrel cage. When the DC supply is disabled and the machine is operating at less than synchronous speed, this winding receives induced voltage from the stator by Faraday's law and generates a magnetic field through the current that flows through its short-circuited bars. When the machine is running at synchronous speed, this voltage is no longer induced because there is no relative motion between the stator and rotor flux. The field winding's operation depends on the state of the operation switch. In induction start mode the field winding is short circuited to improve the machine's starting torque and assist the machine's operation as an induction motor. When the machine is in synchronous run mode, the field winding is connected to the DC excitation and serves as the source of rotor flux. To measure the resistance of the machine, a DC source was connected across the DC input terminals with the SM-100 in synchronous run mode and no other system inputs being applied to the machine. Using ohm's law to calculate the voltage across the terminals, the rotor field resistance was found to be 102 Ω. This value is the resistance of the field winding as the damper winding is short circuited.

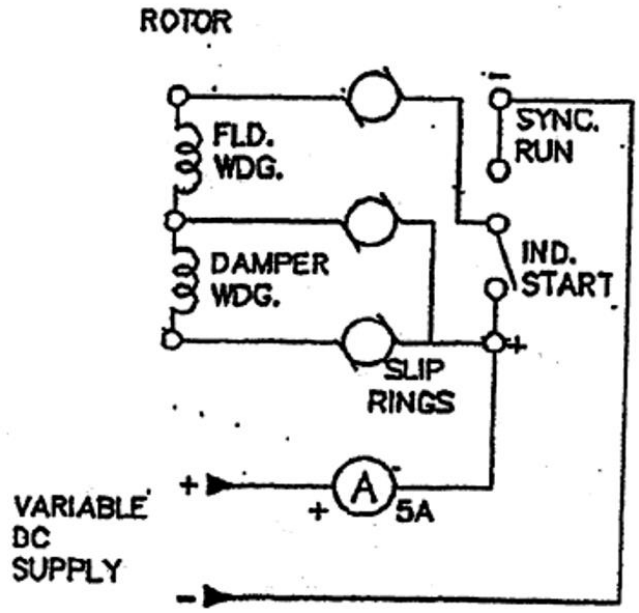

Figure 23: SM-100 Rotor Winding Configuration

To determine the parameters of the rotor damper winding, two different locked rotor experiments were completed. Under the locked rotor test condition, a large load torque is placed on the machine to prevent the rotor from rotating. In this condition, the slip of the machine is 1 and the damper and field windings have the maximum reflection into the stator. In the first experiment, the DC excitation was left as an open circuit and the machine operation switch was turned to induction start mode. In this mode, the rotor field windings become short circuited to help provide the machine with starting torque. The input voltage was provided with an autotransformer to adjust the current to the rated value as is traditionally done for short circuit tests. In the second experiment, the DC excitation was left as an open circuit and the machine operation switch was turned to synchronous run mode. The autotransformer position was not adjusted, and thus the input voltage remained the same. This configuration opens the rotor field winding circuit and leaves the damper windings to produce the magnetic field of the rotor. Without the DC excitation, the machine operates as an induction machine even though it is in synchronous run mode. The starting torque of the SM-100 was measured for both experiments using the Magtrol dynamometer. Out of the two experiments, the synchronous run operation without a DC excitation produced less starting torque because the field winding is not short circuited to receive an induced voltage. When the torque was measured for both cases, it was found that the starting torque of the 2nd experiment was approximately 64% of the starting torque of the first experiment. This implies that the starting torque provided by the damper winding is almost twice that of the starting torque provided by the field winding when the machine is in induction start mode. The schematic used for these experiments can be seen in Figure 24.

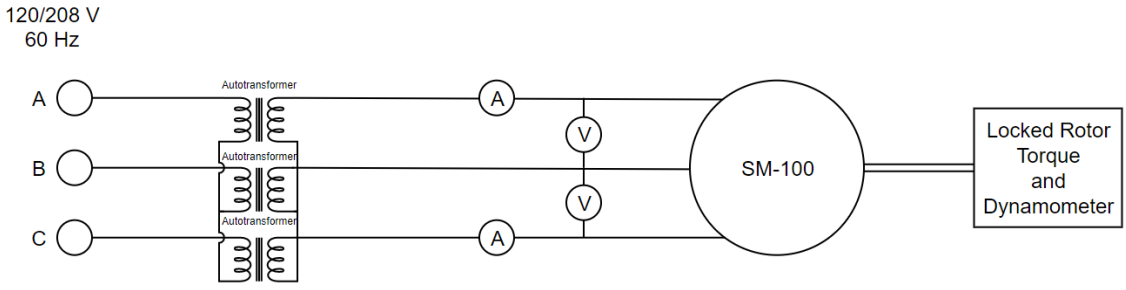

Figure 24: Locked Rotor Damper Winding Measurement Schematic

Using the results of the synchronous run operation and induction start operation experiments, the value of R_{Damper} can now be calculated. The experiment that was completed in induction-start mode uses the machine as an induction motor with both the damper and field windings in use, while the synchronous-run experiment conducted leaves the machine operating as an induction machine due to the open circuiting of the field coil. The real power of each case and the known value of R_{Field} can be used to calculate the R_{Damper} value of 135 Ω using Table 5 and the equations below.

Table 5: Rotor Parameters Measurement by Locked Rotor at Rated Current Output Data

Case	V_{LL} (V)	I_A (A)	P 3ϕ (W)	S 3ϕ (VA)	Q 3ϕ (VAR)	PF	Torque (Lb-in)
Induction Start	67.9	1.717	117	201.9	164.6	0.579	3.5
Synchronous-Run	64.5	0.774	47.3	86.5	72.4	0.547	1.8

$$From\ the\ preliminary\ core\ loss\ experiment: \mathrm{P_{coreloss}} = 54\ (W)\ for\ V_{LL} = 209\ (V)$$

$$P_{3\varphi-2coils-core\ loss} = \left(\frac{67.9}{209}\right)^2 * 54(W) = 5.7\ (W) \tag{26}$$

$$P_{3\varphi-one\ coil-core\ loss} = \left(\frac{64.5}{209}\right)^2 * 54(W) = 5.14\ (W) \tag{27}$$

$$P_{3\varphi-2\ coils-stator\ loss} = 3(4.3\Omega)(1.717^2) = 38\ (\mathrm{W}) \tag{28}$$

$$P_{3\varphi-one\ coil-stator\ loss} = 3(4.3\Omega)(0.774^2) = 7.7\ (W) \tag{29}$$

$$P_{3\varphi-2\ coils-net} = 117 - 5.7 - 38 = 73.3(W) \tag{30}$$

$$P_{3\varphi-damping\ coil-net} = 47.3 - 5.14 - 7.7 = 34.5(W) \tag{31}$$

$$P_{rotor-field\ coil} = P_{3\varphi-2\ coils-net} - P_{3\varphi-damping\ coil-net} = P_{3\varphi-\text{field coil}} = 73.3 - 34.5 = 38.8\ (W) \quad (32)$$

$$P_{rotor-field\ coil} = R_{field} * I_{induced\ field\ coil}\text{^}2 = (102\Omega)(I_{induced\ field\ coil})\text{^}2 = 38.8\ (W) \quad (33)$$

$$I_{induced\ field\ coil} = 0.62\ (A) \quad (34)$$

$$From\ a\ locked\ rotor\ experiment: I_{induced\ field\ coil-measured} = 0.66\ (A)\ for\ I_a = 1.807\ (A)$$

$$I_{induced\ field\ coil-calculated} = \left(\frac{1.717}{1.807}\right)(0.66) = 0.63\ (A) \quad (35)$$

$$P_{rotor-damping\ coil} = R_{damping} * (I_{induced\ damping\ coil})^2 = 34.5\ (W) \quad (36)$$

$$The\ ratio\ of\ \frac{P_{rotor-damping\ coil}}{P_{rotor-field\ coil}} = \frac{34.5(W)}{38.8(W)} = 0.89 \quad (37)$$

$$The\ ratio\ of\ \frac{(I_{stator-damping\ coil})^2}{(I_{stator-field\ coil})^2} = \frac{(0.774)^2}{(1.717-0.774)^2} = 0.67 \quad (38)$$

$$The\ ratio\ of\ \frac{R_{damping\ coil}}{R_{field\ coil}} = \frac{0.89}{0.67} = 1.33 \quad (39)$$

$$R_{damping\ coil} = (102\Omega)\left(\frac{0.89}{0.67}\right) = 135(\Omega) \quad (40)$$

$$P_{rotor-damping\ coil} = R_{damping} * (I_{induced\ damping\ coil})^2 = (135\Omega)(I_{induced\ field\ coil})^2 = 34.5\ (W) \quad (41)$$

$$I_{induced\ damping\ coil} = 0.505\ (A)$$

To gain insight into the configuration of the rotor windings of the SM-100, experiments were conducted to specifically consider the stability of the power drawn by the SM-100 under various testing conditions. For this experiment two SM-100s synchronous machines were coupled, with one machine configured as a motor and the other machine configured as a mechanical load. For this analysis three different test cases will be examined. The first test case to be examined is with the motor in synchronous run operation with an applied DC input. In this mode, the machine operates as a synchronous motor and thus the input power being consumed

is held constant throughout the 60 Hz cycle. The second test case to be examined is with the motor in synchronous run operation, but without an applied DC input. In this mode, the machine operates as an induction motor with the field winding open circuited. This open circuit DC condition results in massive fluctuations in the power drawn by the machine, with the input power oscillating by as much as 60 W. The third and final test case has the motor configured in induction start mode. This induction-start condition results in slight fluctuations with the input power for each cycle oscillating by as much as 10W. These results show that the SM-100 is a salient pole machine and is configured as shown in Figure 26. When the machine is in synchronous mode with an applied DC input, the principles of an induction machine are not relied on and thus the machine operates without fluctuations in the input power. This changes however when the machine is run as an induction motor as the machine now achieves rotation due to the induced voltage in the short-circuited rotor windings. An ideal squirrel cage induction motor would have the copper bars of the squirrel cage completely enclosing the rotor, but that is not possible for the SM-100 as the field windings must be added for synchronous run operation. For the induction start case, oscillation is minimized as within the angular positions at which the copper bars are not present on the rotor, field windings are present and short circuited. This helps to improve the relative stability of the input power that the machine draws. For the synchronous run case with no DC input, the field windings are open circuited and thus do not allow for generation of magnetic field. This gap in the rotor makes the machine unstable and results in the significant variation of input power drawn by the motor.

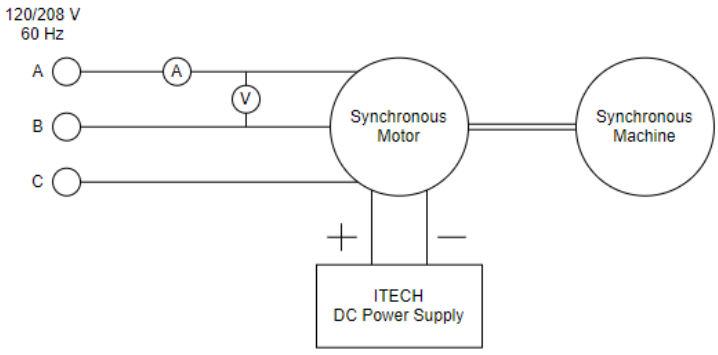

Figure 25: Experimental Schematic for Rotor Winding Configuration Experiment

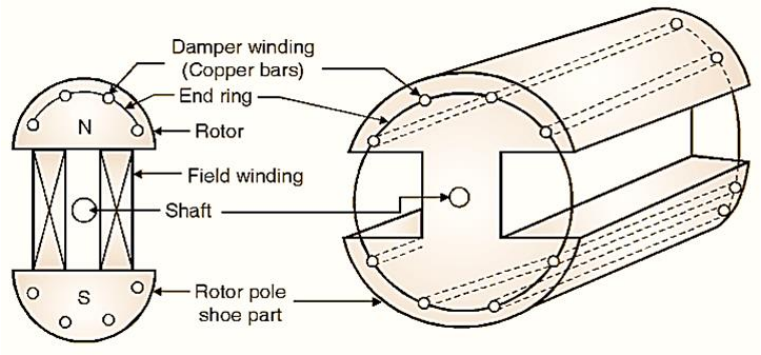

Figure 26: Rotor Winding Configuration [9]

5.5 Stator Rotor Turns Ratio

The turns ratio of a synchronous machine is a critical parameter to identify as it influences the reflected impedance the stator and rotor see from each other. The turns ratio can be calculated by dividing the number of turns in the stator winding by the number of turns in the rotor field winding [10]. To determine the turns ratio of the synchronous machine, the machine was once again set up as a motor in the locked rotor test condition and underwent an experiment in synchronous run mode.

$$Turns\ Ratio = n = \frac{Number\ of\ Stator\ Winding\ Turns}{Number\ of\ Rotor\ Winding\ Turns} \tag{42}$$

In this experiment, the SM-100 was run as an induction motor in synchronous run mode, but with the field winding short circuited through an ammeter under a locked rotor test condition. With the machine in this configuration, the motor behaves like a transformer with an air gap as both a transformer and a locked induction motor have a slip of 1 and produce no mechanical power output. With the machine in induction run mode, the damper and field windings of the synchronous machine are placed in parallel such that both windings can contribute to the torque of the machine. The machine under test was sourced from three-phase AC power and the input stator current and induced field winding current were measured. The AC power provided to the machine was set at low voltage using an autotransformer to ensure that the core losses of the machine would be negligible. When the stator input was measured to be 270mA, the current through the field winding was measured to be 90mA. Using equation 43 and these measured values, a turns ratio of 0.333 can be calculated. This turns ratio represents the relationship between the stator coils and the rotor field winding. A turns ratio considering the rotor damper windings could not be calculated as the damper windings are always short-circuited. Fortunately, the damper winding turns ratio is not required to understand the SM-100's behavior at synchronous speed, as at synchronous speed the slip of the rotor is zero and the machine is unaffected by the damper windings.

$$I_{stator} = \frac{I_{field}}{n} \tag{43}$$

5.6 Stator to Rotor Mutual Inductance Experiment

In this experiment the SM-100 synchronous machine was set up as a motor under a locked rotor test condition with the motor in synchronous run mode to measure the effect of mutual inductance from the stator to the rotor field winding. The input to the synchronous motor was from an autotransformer and the measured data points were the stator AC voltage and current and the field winding's voltage with the field winding open circuited. To conduct the experiment, the input stator voltage was adjusted through the autotransformer. This provided a source to generate current through the stator windings and induce voltage in the rotor windings. The schematic for this experiment can be seen in Figure 27 and the full results from this experiment can be found in Appendix C.

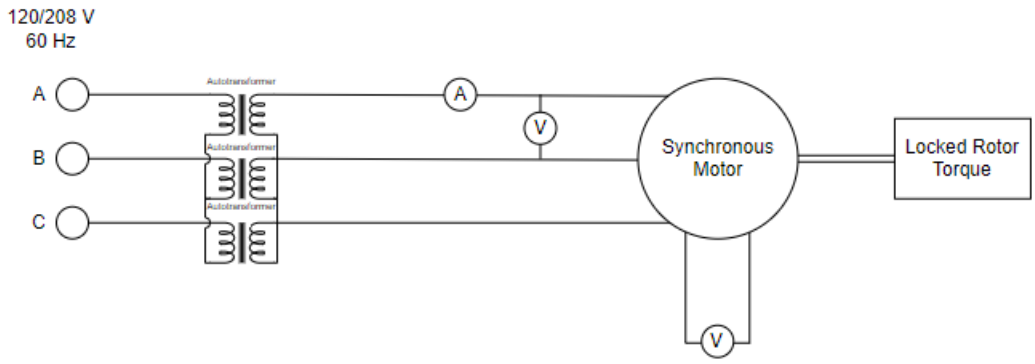

Figure 27: Stator to Rotor Mutual Inductance Experiment Schematic

The output data for this experiment clearly shows the point at which the machine reaches the knee of the BH curve of the core material. The induced voltage follows a linear trajectory until the induced voltage reaches approximately 60 V. At this point the relationship between I_{AC} and the rotor induced voltage becomes nonlinear. The linear component of the output data is plotted in Figure 28. As the experiment occurs in the locked rotor test condition, the induced electrical frequency in the rotor is 60 Hz and the machine's slip is 1. Using the slope of the equation of the linear trendline, we can estimate the constant $K_{S\text{-}F}$ to be 0.247 for voltage induced from the stator to the rotor field winding. It is important to note that while the field winding of the rotor is open

circuited, the damper winding is always short circuited and thus is still producing a magnetic field that interacts with the magnetic field being produced by the stator. Thus, this constant $K_{S\text{-}F}$ considers the impact of both the stator field coils and the rotor damper winding on the rotor field winding.

$$\mathrm{E_{ind}} = \mathrm{I_{AC}} * \mathrm{w_s} * \mathrm{K_{S-F}} \tag{44}$$

$$\frac{E_{ind}}{\mathrm{I_{AC}} * \omega_{\mathrm{mechanical}}} = K_{S-F} = 0.247 \frac{V}{A * \frac{rad}{s}} \tag{45}$$

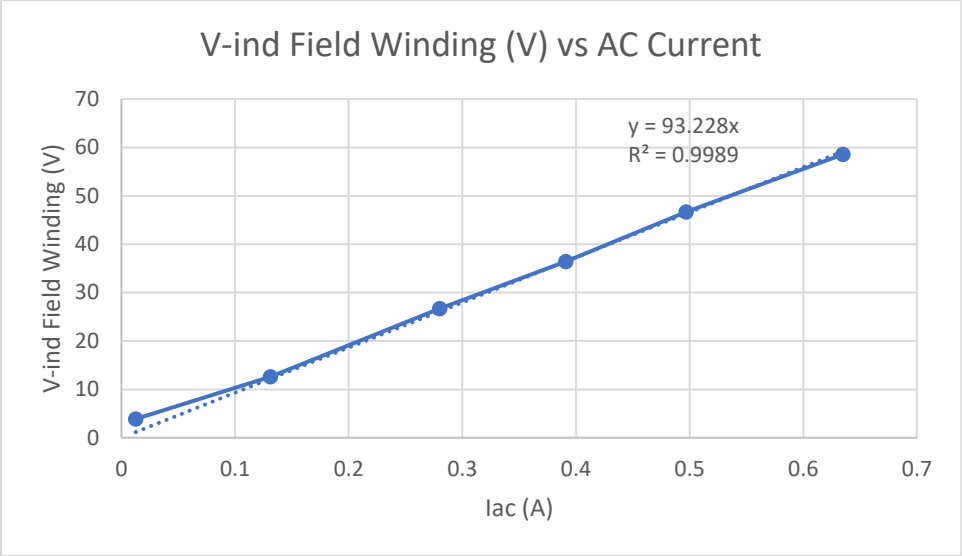

Figure 28: Linear Field Winding Induced Voltage vs Stator Current

5.7 Open Circuit Test

A synchronous generator open circuit test was conducted on the Hampden SM-100 as the first step to define the synchronous reactance of the machine using the classical approach. In this test the SM-100 under test was setup as a generator and received its input power through its coupling to an additional SM-100 that was running as a synchronous motor. The stator windings of the synchronous generator under test were left open and their line voltage was measured as the excitation current to the rotor was varied with the ITECH DC power supply. The data from the open circuit test will be used with the results of the short circuit test to calculate the synchronous reactance of the SM-100. The full results from this experiment can be found in Appendix D.

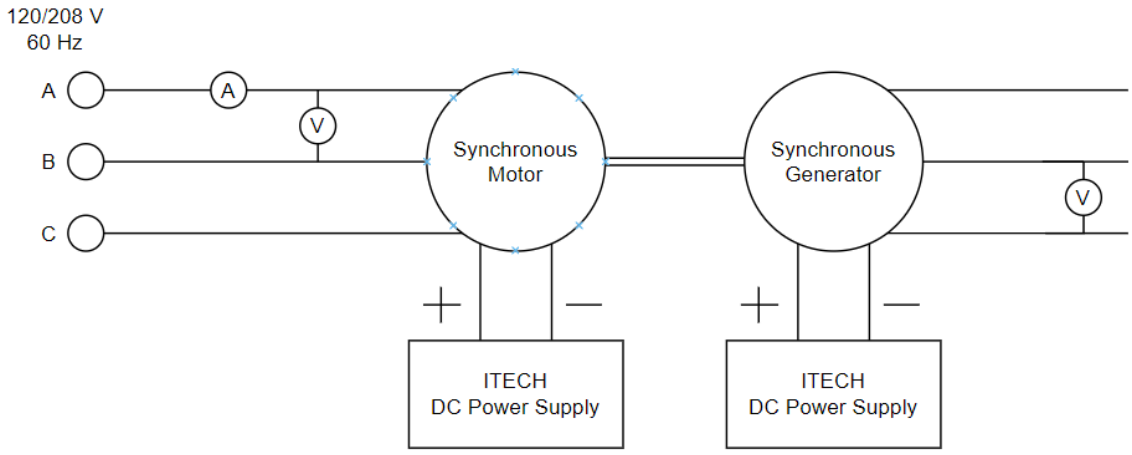

Figure 29: Open Circuit Test Experiment Schematic

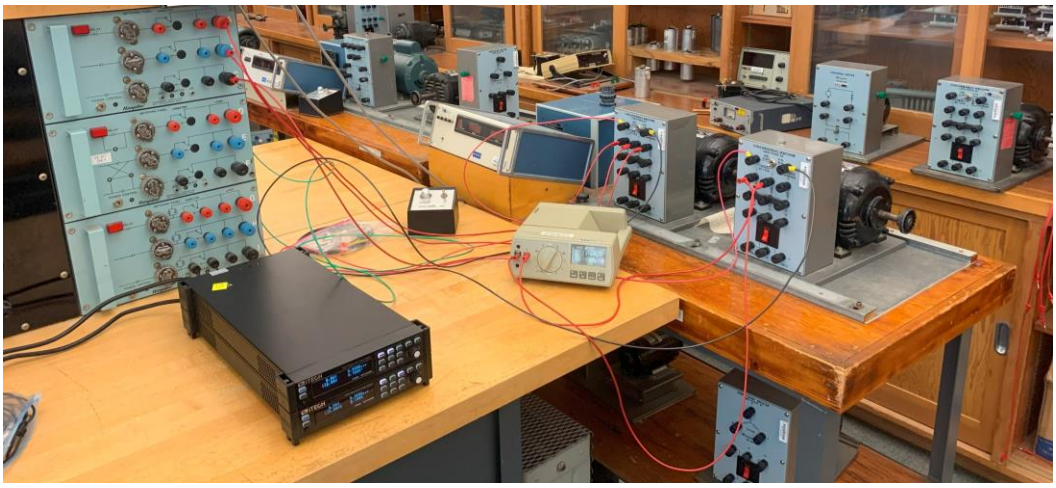

Figure 30: Open Circuit Test Experimental Setup

The data collected from the open circuit test can be seen in the stator line voltage vs excitation current curve of Figure 31. In the plot the stator line voltage increases linearly with the excitation current until the excitation current reaches 0.4 A. This behavior is emphasized in Figure 32 where the stator line voltage vs excitation current curve is reduced to show the excitation current from 0 A to 0.4A. After 0.4 A, the stator line voltage continues to increase, but does so in a decaying rate. This behavior is emphasized in Figure 33 where the stator line voltage vs excitation current curve is reduced to show the excitation current from 0.4 A to 0.6 A. This decay can be attributed to the core reaching the knee of its BH Curve and thus having an increasing reluctance. This experiment could not be continued at higher excitation currents due to the voltage rating of the machine, but if the excitation current was continued to be increased, the permeability of the core would have eventually been reduced to the permeability of air.

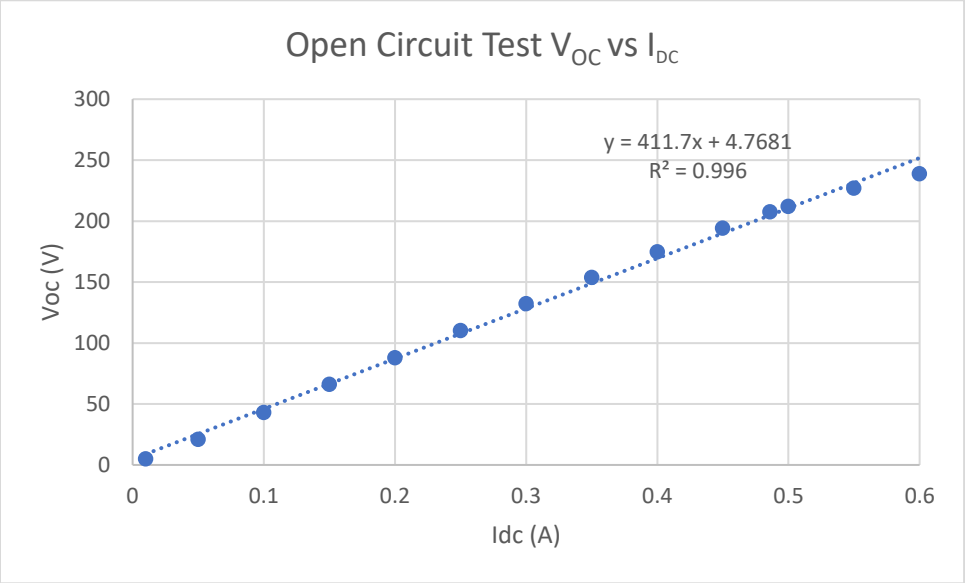

Figure 31: Full Open Circuit Test Stator Line Voltage vs Excitation Current Curve

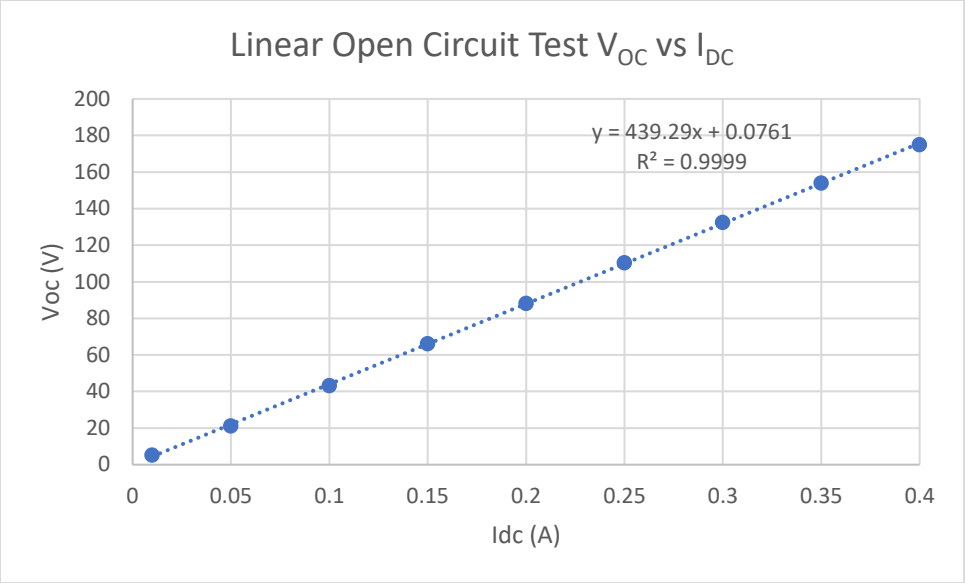

Figure 32: Linear Open Circuit Test Stator Line Voltage vs Excitation Current Curve

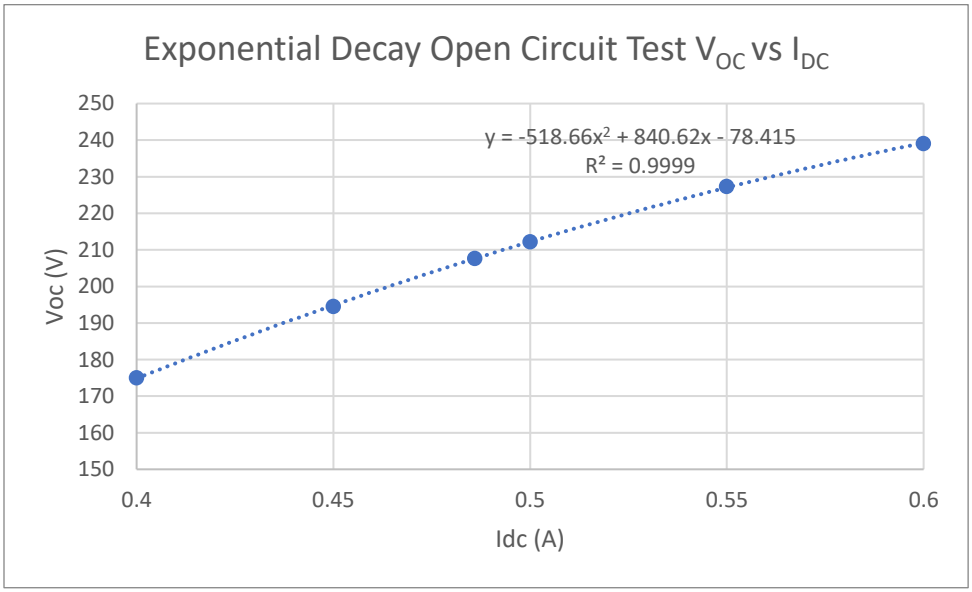

Figure 33: Exponential Decay Open Circuit Test Line Voltage vs Excitation Current Curve

5.8 Short Circuit Test

A synchronous generator short circuit test was conducted on the Hampden SM-100 as the second step to define the synchronous reactance using the classical model for synchronous machines. The SM-100 under test was set up as a generator and received its input power through its coupling to an additional SM-100 that was running as a synchronous motor. The stator windings of the synchronous generator under test were short circuited and their line current was measured as the excitation current to the rotor was varied with the ITECH DC power supply. The data from this short circuit test will be used with the results of the open circuit test to calculate the synchronous reactance of the SM-100. The full results from this experiment can be found in Appendix E.

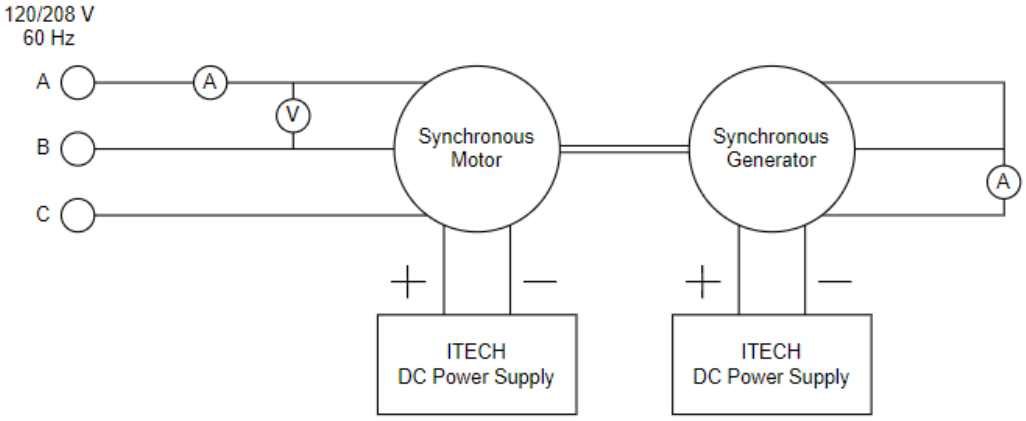

Figure 34: Short Circuit Test Experiment Schematic

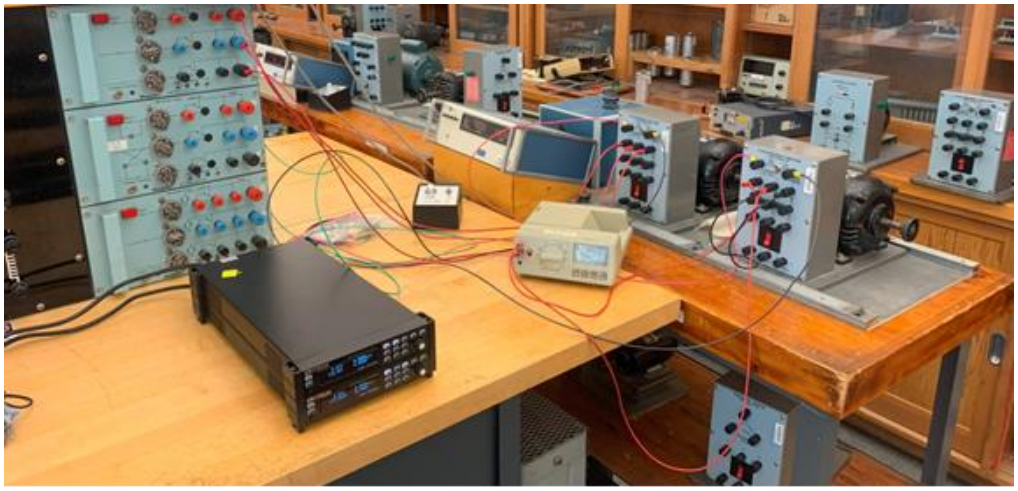

Figure 35: Short Circuit Test Experimental Setup

The data collected from the short circuit test can be seen in the stator line current vs excitation current curve of Figure 36. In the plot the stator line current increases linearly with the excitation current. This plot remains linear as, unlike in the open circuit test, the short circuit test condition does not cause saturation in the machine. The value of synchronous reactance is calculated in section 6.1 of this report.

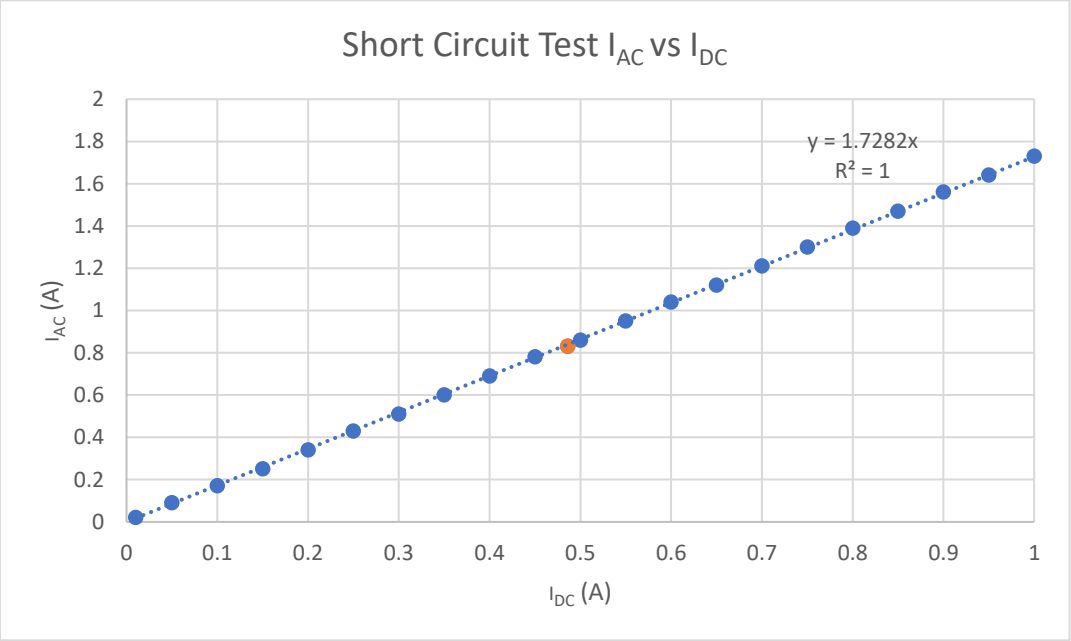

Figure 36: Short Circuit Test AC Current vs DC Current Curve

5.9 Loaded Generator Test

A loaded synchronous generator test was conducted on the Hampden SM-100 to determine the synchronous generator's behavior under load. In this test the SM-100 under test was set up as a synchronous generator and received its input power through its coupling to an additional SM-100 that was running as a synchronous motor. Each phase of the stator windings of the synchronous generator under test were connected to a load of 2 35 Ω resistors and 2 30mH inductors in series. During the experiment, the excitation current was varied via the ITECH DC power supply to determine how the system responded to different excitation currents. The full results from this experiment can be found in Appendix F.

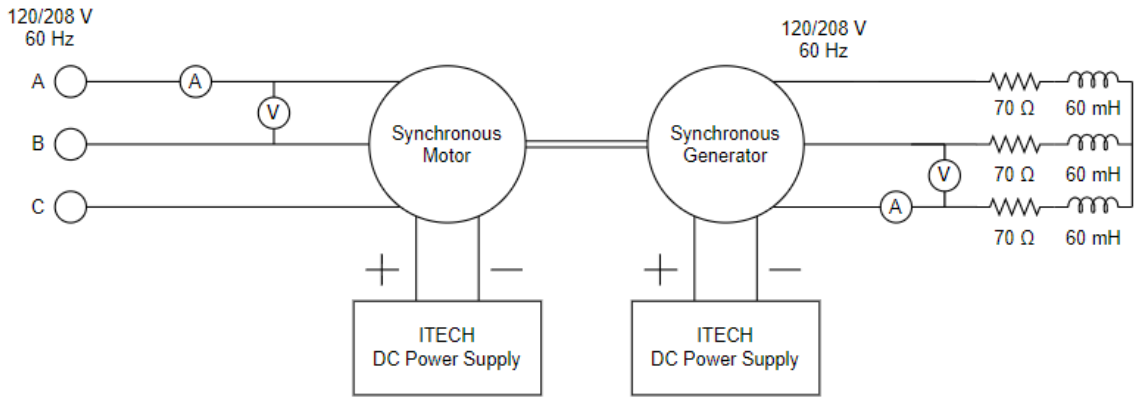

Figure 37: Loaded Generator Test Experiment Schematic

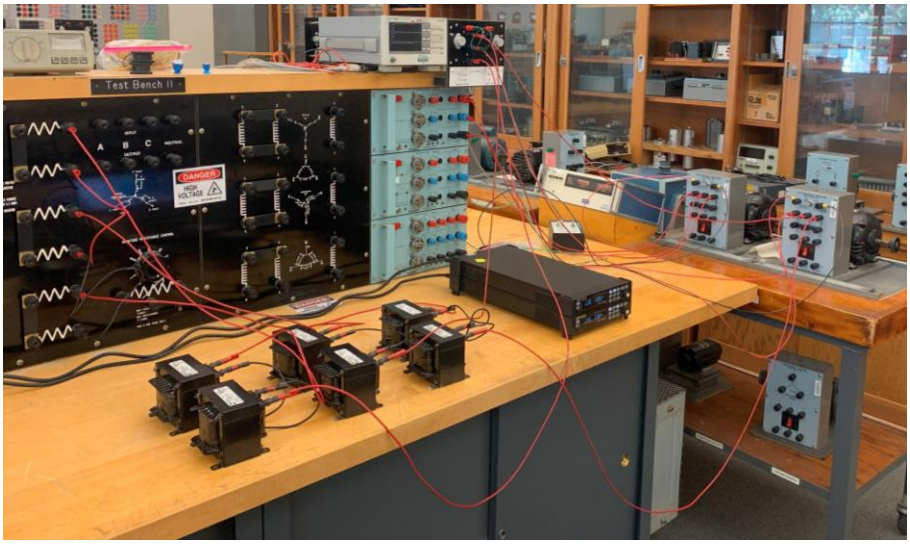

Figure 38: Loaded Generator Test Experimental Setup

This experiment creates an opportunity to calculate the constant K for the induced voltage into the stator windings from the magnetic field of the rotor. As can be seen in Figure 39, the relationship between the excitation current and the induced voltage in the stator windings follows a linear trajectory for all recorded data points. Using the mechanical frequency and the slope of the linear relationship found in Figure 39, the constant $K_{R\text{-}S}$ can be calculated using equation 47. This constant represents many parameters within both the stator and the rotor such as the number of turns in the rotor and the radius of the coils of the stator pole. Using the slope of the equation of the linear trendline, we can calculate the constant $K_{R\text{-}S}$ to be 0.566 for voltage induced from the rotor to the stator.

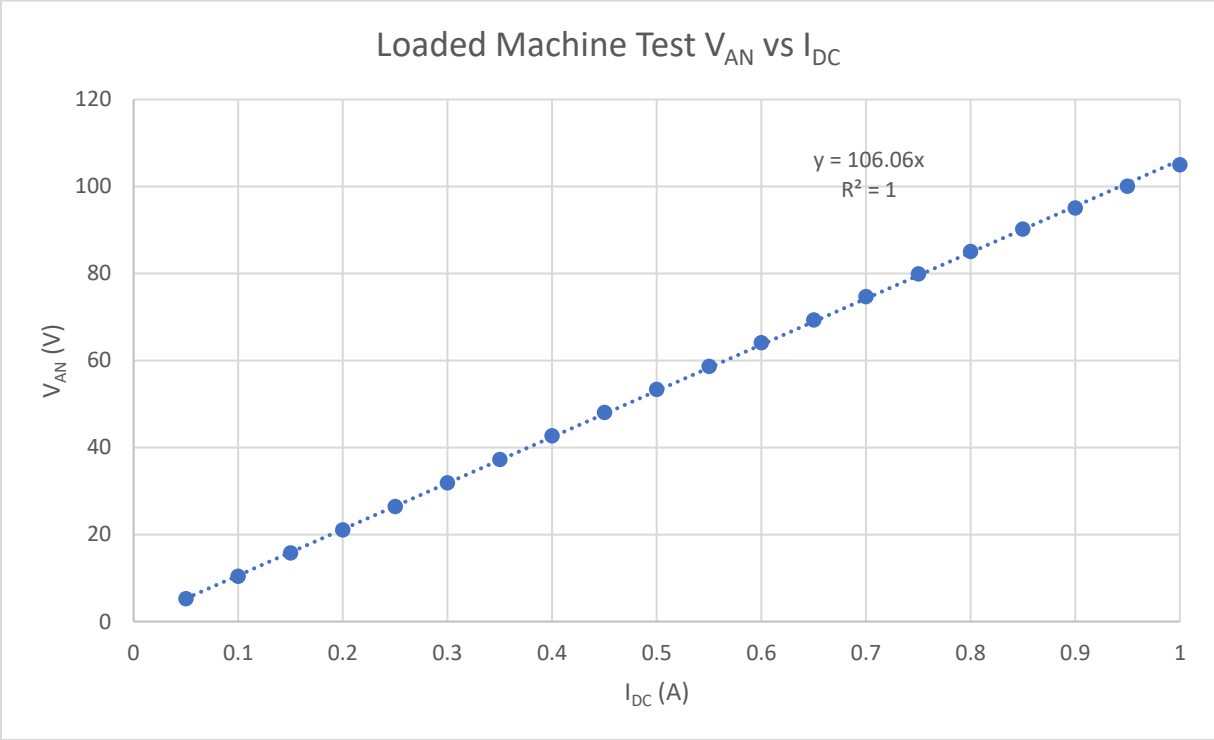

Figure 39: Loaded Generator Test V_{AN} vs I_{DC} Plot

$$\mathrm{E_{ind}} = \mathrm{K_{R-S}} * \mathrm{I_{DC}} * \omega_{\mathrm{mechanical}} \tag{46}$$

$$\frac{E_{ind}}{\mathrm{I_{DC}} * \omega_{\mathrm{mechanical}}} = K_{R-S} = 0.566 \frac{V}{A * \frac{rad}{s}} \tag{47}$$

5.10 Generator Capability Curve

A synchronous generator capability curve is used to determine the limits that a generator can be safely operated without exceeding its rated parameters. An example of a generator capability curve can be seen in Figure 40. To create a generator capability curve for the SM-100, the machine was set up as a generator and received its input power through its coupling to an additional SM-100 that was running as a motor and acting as the prime mover. The stator windings of the synchronous generator under test were connected to varying loads that ranged from completely resistive to completely inductive. The data from these tests were used to make the generator capability curve in Figure 43. The full data tables from this experiment can be found in Appendix G.

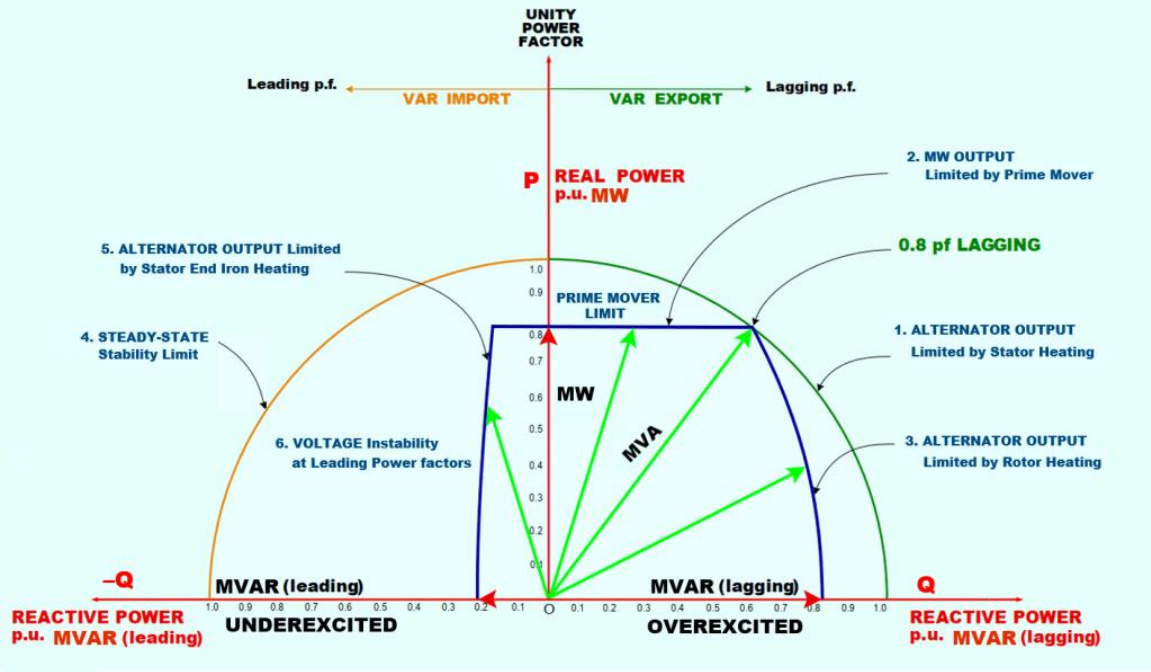

Figure 40: Example Generator Capability Curve [11]

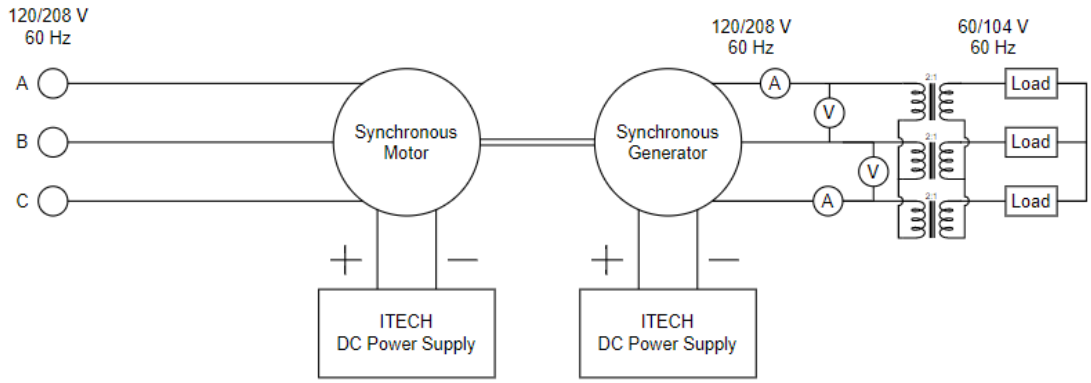

Figure 41: Generator Capability Curve Experiment Schematic

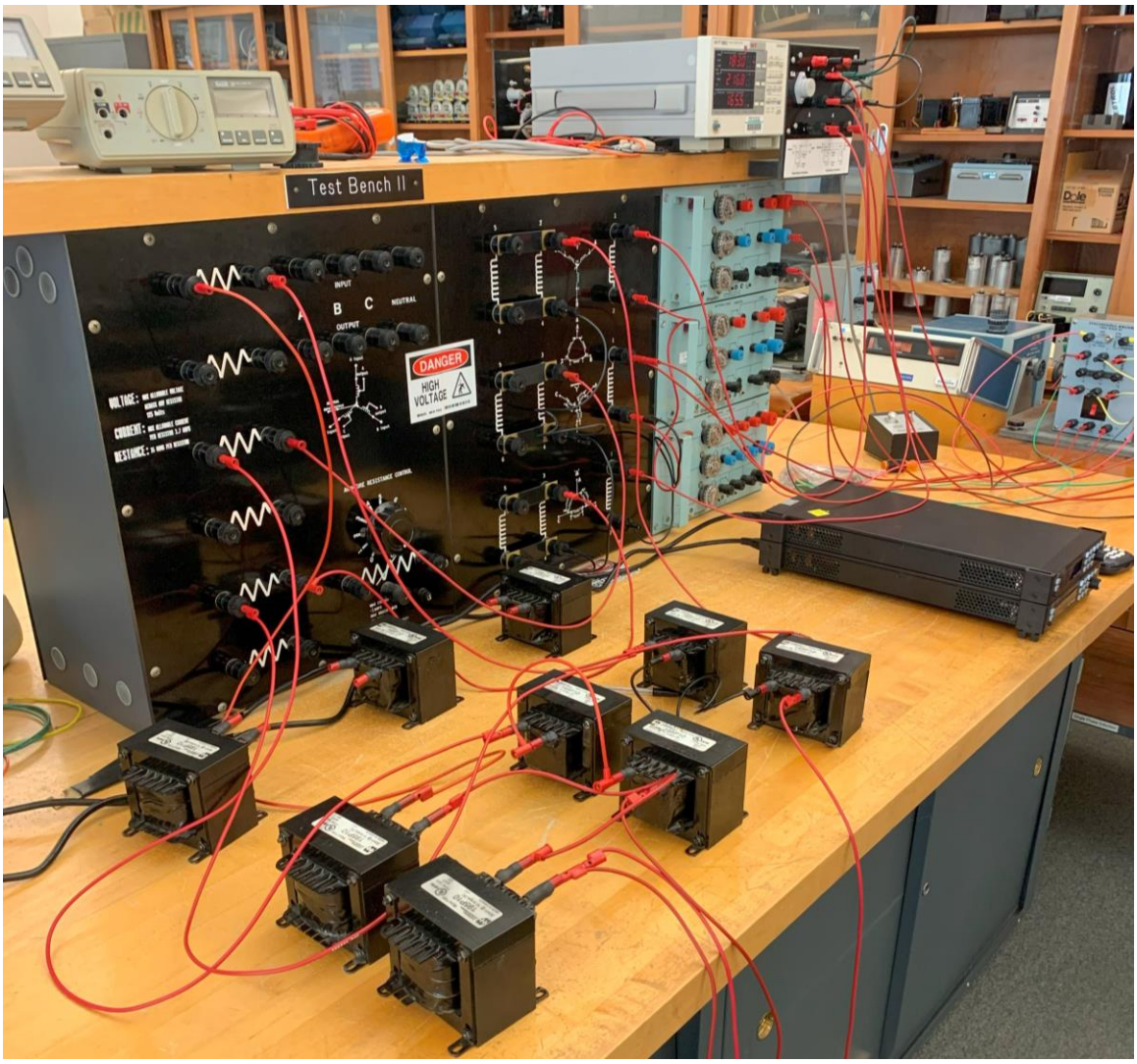

Figure 42: Generator Capability Curve Loading Experimental Setup

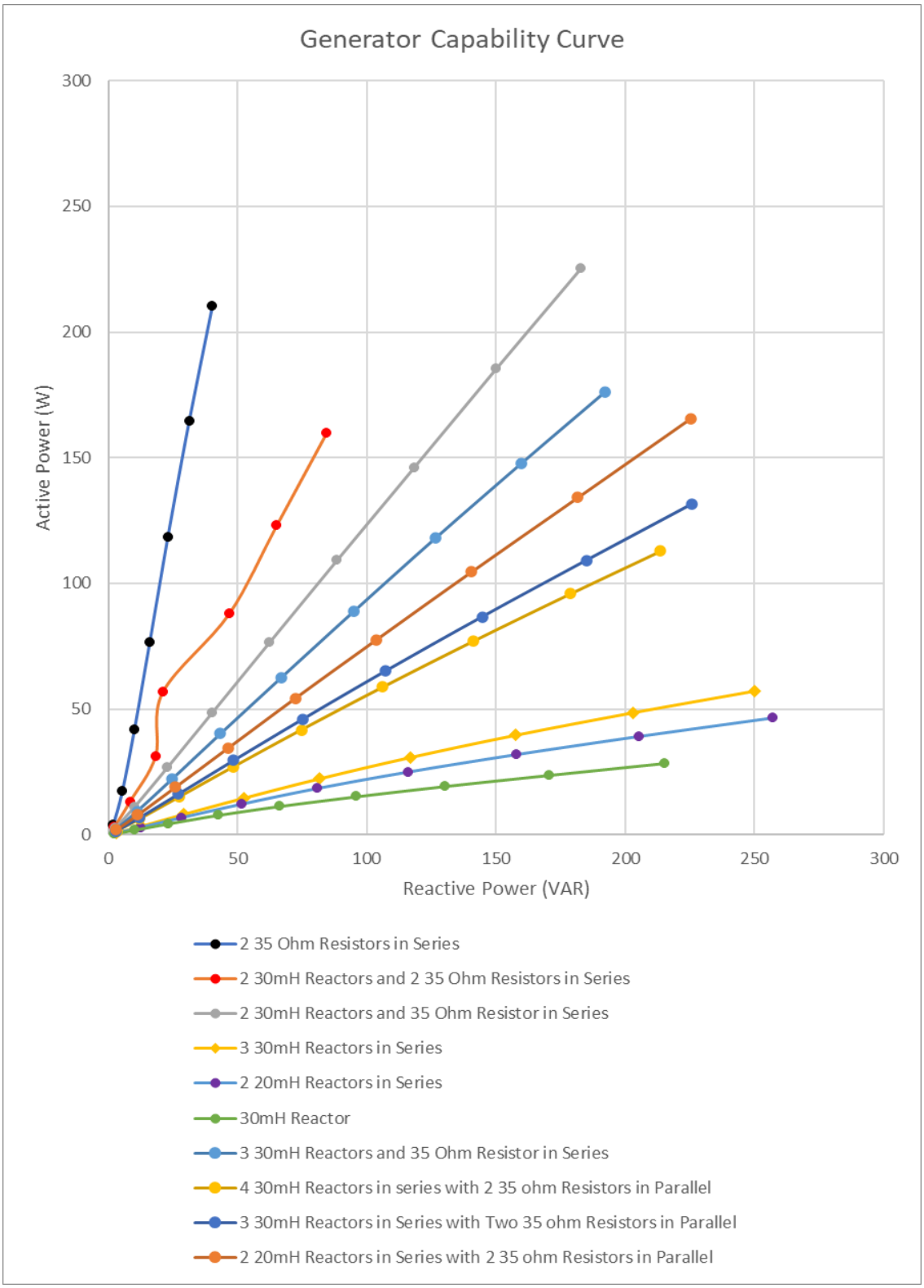

Figure 43: Generator Capability Curve

The created generator capability curve for the SM-100 has a similar shape to the example generator capability curve given in Figure 40. The curve is limited by the excitation current, voltage rating, the load current rating, and the maximum power output of the machine. Table 6 summarizes the most important datapoints from this curve by identifying the maximum real power, maximum reactive power, maximum apparent power, maximum power factor, and minimum power factor datapoints.

Table 6: Summary of Key Generator Capability Curve Data Points

	Test Case	Generator Excitation Current (A)	Real Power (W)	Reactive Power (Q)	Apparent Power (S)	Power Factor
Maximum Real Power	2 Reactors and 1 Resistor	0.9	225.4	183	290.3	0.776
Maximum Reactive Power	2 Reactors	0.6	46.4	257.3	261.7	0.177
Maximum Apparent Power	2 Reactors and 1 Resistor	0.9	225.4	183	290.3	0.776
Maximum Power Factor	2 Resistors	0.9	164.6	31.4	166.7	0.9874
Minimum Power Factor	1 reactor	0.9	28.3	218.6	215.2	0.129

5.11 Intermediate Core and Reactance Parameter Measurement

When the SM-100 is operating in induction-start mode, the rotor's field winding and damper winding are short circuited to generate a magnetic field in the rotor. For this magnetic field to be created, the rotor must be rotated at less than synchronous speed or voltage will not be induced in the rotor windings by the principles of Faraday's law. When attempting to measure the synchronous machine's stator and core parameters it is difficult to separate the rotor winding parameters from the stator and the core. For this experiment, an SM-100 was configured as a synchronous motor and used as a prime mover for a second SM-100 connected to the grid in induction start mode. The schematic for this experimental setup can be seen in Figure 44. As the machine in induction start mode is rotating at synchronous speed, the impedance of the rotor windings is infinite as the slip has been set to 0. This means the SM-100 is acting as neither a motor nor a generator and that its source only sees the impedance due to the stator and the core. Using the data collected from this experiment and the measured stator resistance of 4.3 Ω, the core resistance of the SM-100 can be calculated to be 761 Ω, using equations 48-51. This value is near to the calculated value of 807.2 Ω from the loaded synchronous motor test earlier in this report. As the power factor is almost zero, the combined equivalent reactance of the stator and the core can also be calculated through equation 52. This equivalent reactance is only true for the induction start case however, as the reactance of the core varies when an excitation current is applied in the rotor field windings. The calculations provided in this section improve upon the values calculated in the preliminary calculations of section 5.3 Preliminary Core Loss Parameter Measurement Experiment, however various simplifications were still made. In this experiment, the reactance of the stator and the variation of the stator resistance with heat were not considered. These factors will be investigated in the following section.

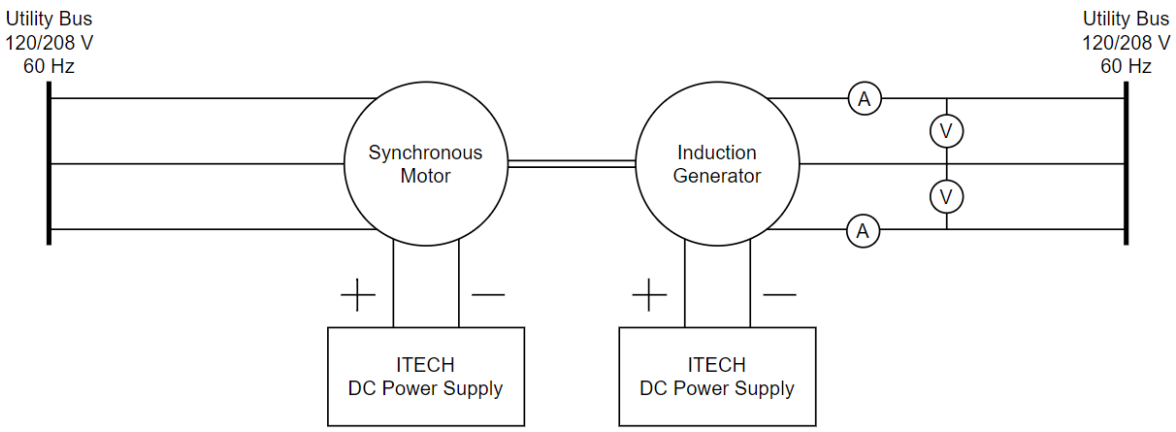

Figure 44: Induction Start Stator and Core Measurement Schematic

Table 7: Induction Start Stator and Core Measurement Data

V_{LL} (V)	I_A (A)	$P_{3\text{-Phase}}$ (W)	$S_{3\text{-Phase}}$ (VA)	$Q_{3\text{-Phase}}$ (VAR)	PF	Speed
209.1	0.838	27.6	303.5	302.1	0.091	1800

$$P_{loss-stator-3Phase} = 3(4.3\Omega)(0.838^2) = 9.1\ (W) \tag{48}$$

$$P_{loss-core-3Phase} = 27.6 - 9.1 = 18.5\ (W) \tag{49}$$

$$Voltage\ across\ the\ parallel\ branch: V_2 = \left(\frac{209.1}{\sqrt{3}}\right) - (\ 4.3\Omega)(0.838) = 117.1\ (V) \tag{50}$$

$$R_{core} = (117.1^2)/(18.5W) = 761\ \Omega \tag{51}$$

$$PF \cong 0 \rightarrow X_s + X_m = X_{eq} = \frac{117.1^2}{302.1\ (VAR)} = 45.4\ \Omega \tag{52}$$

5.12 Temperature Effect on Coil Resistance and Stator Reactance

As the machine operates, the current it is using to create rotation produces heat in the coils of the machine. The coils of the machine are made of copper and the resistance of copper changes with temperature. Copper has a positive temperature coefficient of resistance, and thus its resistance increases as its temperature rises. The rate of change in resistance with temperature is quantified by copper's temperature coefficient of resistance, which is approximately 0.004 per degree Celsius (at 20 degrees Celsius). To calculate this change of resistance, equation 53 can be used with R_0 as the initial resistance at a reference temperature, α as the temperature coefficient of resistance for copper (0.004 per degree Celsius), and ΔT as the change in temperature in degrees Celsius. To measure the initial rotor damper resistance of the machine at room temperature, a DC source was connected across the DC input terminals with the SM-100 in synchronous run mode and no other system inputs. Previously, using ohm's law to calculate the voltage across the terminals, the rotor field resistance was found to be 102.3 Ω. This value is the resistance of the field winding as the damper winding is short circuited in this condition. The variation of the resistance of the damper winding can be identified using the ITECH's VFD display to read the current and voltage for the SM-100 operating as a motor in synchronous run mode. In this condition, the rotor is rotating at synchronous speed and the slip is zero, so the effect of the damper winding is nullified. The full results from all experiments in this section can be found in Appendix H.

To measure the increase of resistance, an experiment was conducted on a SM-100 acting as a synchronous motor with the excitation current held constant at 0.9 A DC while torque was increased from 0 to 12.15 Lb-in. As the experiment progressed and the coils continued to heat up, the DC resistance of the machine increased to as high as 115.1 Ω. Using equation 53 and assuming a room temperature of 20 °C, this would correspond to a temperature increase of 31.3 °C. This increase in resistance will directly increase the power loss in the rotor as copper loss is directly proportional to resistance. A similar effect will be seen in the stator coil but cannot be measured directly. Thus, an approximation of the increase in stator resistance was used by

defining a heat factor variable and applying it to the known stator resistance as seen in equation 54 and equation 55. These equations use the assumption that the heat increase within the machine is uniform.

$$\Delta R = R_0 * \alpha * \Delta T \tag{53}$$

$$\text{Heat Factor} = HF = \frac{R_{dc-measured}}{R_{dc-nominal}} \tag{54}$$

$$R_{stator-new} = R_{stator-old} * HF \tag{55}$$

The data from the synchronous motor heat variation experiment can also be used to calculate the value of the stator reactance. To estimate this value, the square of the input AC current was plotted against the reactive power in Figure 45. This relationship generated a linear trendline that contains an offset of -117.83 VAR and a slope of 52.348 Ω to multiply by the square of the current to calculate the single-phase reactive power. Due to the relationship between the square of the current and the reactive power generated by a series reactance element, the slope was defined to be the combination of the series reactance of the rotor and the stator, and the offset was defined to be the reactive power required to magnetize the core of the machine. As the machine is acting at 0.9 A DC and has a leading power factor this offset is negative due to excess VARs being provided by the rotor excitation current. As a preliminary estimation, the reactance of the stator and rotor was picked to be equivalent such that each parameter had a value of 26.174 Ω. The validity of this estimation will be explored in the next experiment conducted in this section.

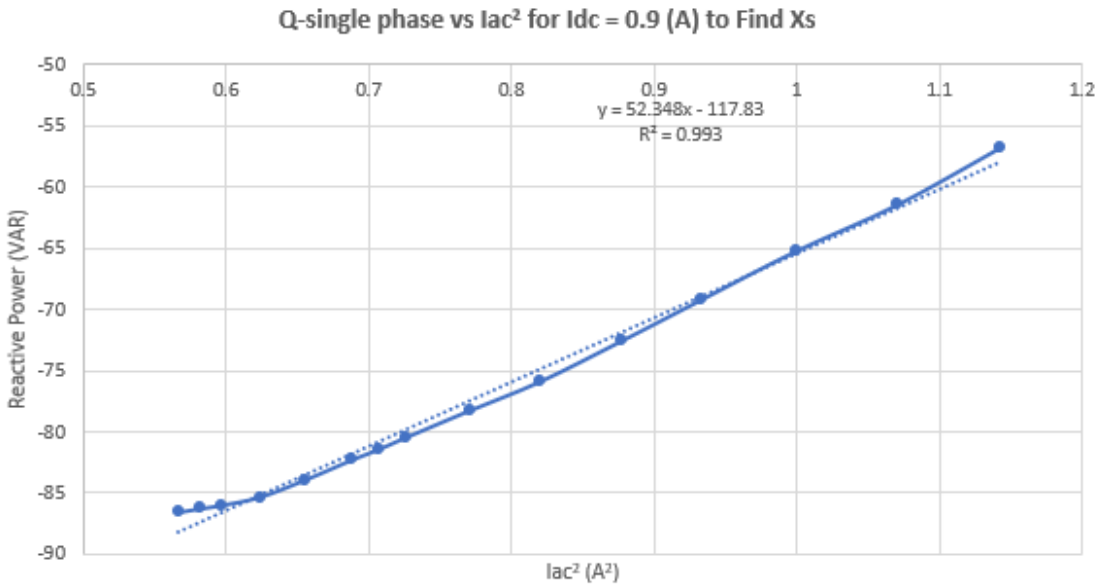

Figure 45: Single Phase Reactive Power vs I_{AC} for I_{DC}=0.9A

$$Q_{core-0.9A\ DC-1Phase} = -117.83\ VAR \tag{56}$$

$$X_{stator+rotor} = 52.348\ \Omega \tag{57}$$

$$X_{stator} = X_{rotor} = \frac{X_{stator+rotor}}{2} = 26.174\ \Omega \tag{58}$$

As a test to confirm the validity of the assumption that the stator reactance is equal to the rotor reactance, the calculated value of 26.174 Ω was applied to an additional experiment. In this experiment, an SM-100 was set up as a synchronous motor while torque was increased from 0 to 11.88 Lb-in. Unlike the previous experiment, the excitation current was increased with each step increase in torque such that the power factor from the AC input was as close to 1 as possible. The power factor value of 1 was selected to simplify the calculations and assume that the phase angle between the stator and rotor voltage is zero. Using the collected data from the experiment, the voltage drop across the core of the machine and the phase angle, δ, between the voltage across the core and the input ac voltage were calculated using equation 59 and 60 respectively. These values were used with the calculated stator reactance value to calculate the three-phase power consumed by the machine. In comparing this value to the measured value of consumed three-phase power, the maximum percent error was 1.47%. This low percent error shows that

the calculated X_{stator} value is accurate, and the assumptions made in performing these calculations were correct. As X_{stator} and the V_{core} value that was calculated from Xstator have now been verified to be accurate, V_{core} can be used to calculate a more accurate value of the core resistance. Using equation 63 and taking the average value across all data points, R_c can be calculated to be 770.9 Ω.

$$V_{core} = \sqrt{\left(\frac{V_{LL}}{\sqrt{3}} - I_{ac} * R_{stator} * HF\right)^2 + (I_{ac} * \mathrm{X_{stator}})^2} \tag{59}$$

$$\sin(\delta) = \arctan\left(\frac{I_{ac} * X_S}{\frac{V_{LL}}{\sqrt{3}} - I_{ac} * R_{stator} * HF}\right) \tag{60}$$

$$P_{3Phase-Calculated} = \frac{\frac{V_{LL}}{\sqrt{3}} * V_{core}}{X_{stator}} * \sin(\delta) \tag{61}$$

$$Percent\ Error_{3Phase} = \frac{|P_{3Phase-Calculated} - P_{3Phase-Measured}|}{P_{3Phase-Calculated}} * 100 \tag{62}$$

$$R_c = \frac{V_{core}^2}{P_{core}} \tag{63}$$

To compare the two test cases used to calculate the core resistance, various calculations were completed using the equations below. The AC source efficiency and net AC and DC efficiency of both experiments were calculated using equation 65 and equation 69 respectively. In the second experiment where the excitation was varied to reach the perfectly excited condition, both the AC source and net efficiency of the machine were greater. This is anticipated as the higher excitation current of the constant excitation current case works to increase the hysteresis and eddy current losses in the machine's core and increase the copper loss in both the rotor and the stator. These increased losses decrease the overall efficiency of the machine.

$$P_{mech-3Phase} = n_{RPM} * T_{lb-in} * \frac{1.18}{100} \tag{64}$$

$$AC\ Efficiency = \frac{P_{mech-3\ Phase}}{P_{in-3Phase}} \tag{65}$$

$$Z_s = \sqrt{X_{stator}^2 + (HF * R_{stator})^2} \tag{66}$$

$$\sin(\theta) = -\sqrt{1 - PF^2} \tag{67}$$

$$V_{core} = \sqrt{\left(\frac{V_{LL}}{\sqrt{3}} - I_{ac} * Z_{stator} * PF\right)^2 + (Z_{stator} * I_{ac} * \sin(\theta))^2} \tag{68}$$

$$Net\ Efficiency = \frac{P_{mech-3Phase}}{P_{in-3Phase} + I_{dc} * V_{dc}} \tag{69}$$

The magnetizing reactance of a synchronous machine will vary depending on the dc excitation. When a synchronous machine is running as an under excited synchronous motor, the power factor of the stator input will be lagging, and the magnetizing reactance will be inductive as the stator is sourcing VARs to the machine. Conversely in a synchronous machine that is running as an over excited synchronous motor, the power factor of the stator input will be leading, and the magnetizing reactance will be capacitive as the stator is absorbing VARs from the DC excitation. Due to this variation, the magnetizing reactance cannot be easily modeled for synchronous machines. However, this is not the case with an induction machine. In induction machines the only source of current is in the stator coils and the magnetizing reactance is always inductive. Thus, while the magnetizing reactance of the SM-100 varies in operation as a synchronous machine, a constant magnetizing inductance can be calculated for the SM-100's operation as an induction machine.

To calculate the magnetizing inductance of the SM-100's operation as an induction machine, a no-load test for the induction machine was conducted. As the slip of the machine is very small, the impedance of the rotor seen from the stator is almost an open circuit and thus is ignored for the calculation. Using the calculated X_s value, the V_{core} and Q_{core} can be calculated. These values can be used to calculate the equivalent inductance per phase to be 98.83 Ω using the relationship between the reactance, voltage, and reactive power.

Table 8: Magnetizing Inductance Test Data Table A

V_{LL} (V)	I_{ac} (A)	$P_{3\text{-}Phase}$ (W)	P_{mech} (W)	AC Efficiency	Dyno Friction (W)	$S_{3\text{-}Phase}$ (VA)	PF lagging	RPM (rev/min)
206.5	0.8	66.9	4.1	0.1	0.0	341.6	0.2	1780

Table 9: Magnetizing Inductance Test Data Table B

Torque (Lb-in)	$Q_{3\text{-}Phase}$ (VAR)	$Q_{1\text{-}Phase}$ (VAR)	Xs (Ω)	V_{Core}	Xm (Ω)	Sin(Theta) (degrees)	Zs (Ω)	Slip
0.2	341.0	113.7	26.2	97.3	98.8	-1.0	26.6	0.01

$$\bar{V}_{core} = \bar{V}_a - \bar{I}_a(R_s + jX_s) = \bar{V}_a - \bar{I}_a\overline{Z_s} \tag{70}$$

$$Angle\ of\ I_a = ACOS(pf) = -1.36944\ rad = -78.463\ Degrees \tag{71}$$

$$Angle\ of\ \overline{Z_s} = ATAN\left(\frac{X_s}{R_s}\right) = 1.40812\ rad = 80.68\ Degrees \tag{72}$$

$$\bar{V}_{core} = (119.22\angle 0) - (0.83\angle -78.463)(26.55\angle 80.68) \tag{73}$$

$$\bar{V}_{core} = (97.27\angle -2.217)\ Volts \tag{74}$$

$$Q_{stator-3Phase} = 3\ (0.83)^2(26.2\ Ohms) = 53.76\ VAR \tag{75}$$

$$Q_{core-1Phase} = \frac{340.97 - 53.76}{3} = 95.73\ \ VAR \tag{76}$$

$$X_{m-1Phase} = \frac{97.27^2}{95.73} = 98.83\ \Omega \tag{77}$$

6. MODELING OF SM-100 SYNCHRONOUS MACHINE

6.1 Classical Synchronous Machine Equivalent Circuit Modeling

The initial modeling approach to be considered for the SM-100 is the classical approach. Using equations 78 and 79 and the experimental results from the open circuit and short circuit synchronous generator experiments, the classical model for synchronous machines can be developed. To model the machine for rated voltage, the excitation current value that produces an open circuit test value closest to the rated voltage of the machine may be selected. As the SM-100 is rated 208/120 V, the excitation current value of 0.486 A was selected as this DC current yielded an open circuit line voltage of 207.7 V. In the short circuit test, providing an excitation current of 0.486 A yielded a short circuit current 0.83 A in the stator windings. Using equation 78, this yields a synchronous impedance, Z_s, of 144.47 Ω. By applying a dc voltage across the stator windings, the stator resistance, R_S, was calculated to be 4.3 Ω. Using the values of Z_s and R_s in equation 79, X_s can be calculated to be 144.41 Ω. These results yield the classical model expressed in Figure 46.

$$Z_s = \frac{E_F}{I_{SC}} = \frac{Open\ Circuit\ Per\ Phase\ Voltage}{Armature\ Short\ Circuit\ Current} = \frac{207.7}{\sqrt{3} * 0.83} = 144.47 \tag{78}$$

$$X_s = \sqrt{Z_s^2 - R_s^2} = \sqrt{144.47^2 - 4.2^2} = 144.41 \tag{79}$$

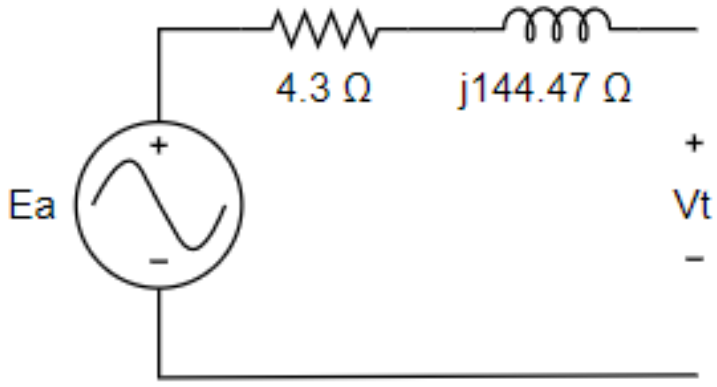

Figure 46: Classical Synchronous Machine Model

6.2 Experimentally Developed Synchronous Machine Model

Throughout the experiments conducted in this thesis, various synchronous machine parameters were calculated. The field winding, damper winding, and stator winding resistance, R_{Field}, R_{Damper}, and R_s respectively, are assumed to remain constant throughout all operating states as they represent the resistance of coils. After performing various tests on the field winding and damper winding, L_{Field} and X_{Damper} were found to vary significantly depending on the operating condition of the machine. As the excitation current and load current increase, the mutual inductance between the stator and rotor coils increases. With this change in inductance that occurs in both the rotor windings, the parameters cannot be given a set value to consistently model the inductance. The magnetizing reactance of the core for synchronous run operation is significantly impacted by the saturation and the level of excitation of the core and thus could not be accurately modeled. A value for the magnetizing inductance could only be calculated for the induction run case where the magnetizing inductance is more constant. The core resistance maintains a much more constant value, and thus, after three iterations of calculations, a final core resistance value was calculated. The full model can be seen in Figure 47. The DC input is shown as a DC current source as all experiments using a DC source were completed with the IT-M3633 in constant current mode so the input DC current to the machine could be used to establish test cases.

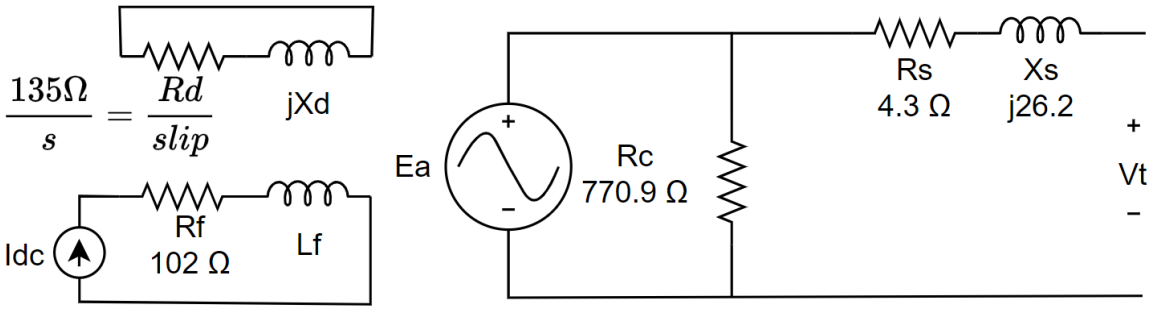

Figure 47: Experimental Developed Synchronous Machine Model

Outside of the equivalent circuit model parameters, significant SM-100 machine characteristics such as the stator to field winding turns ratio, rotor configuration, and the mutual

inductance between the coils of the machine were analyzed. Through a locked rotor test, the stator to rotor field coil turns ratio was determined to be approximately 0.333 by the ratio of stator current to rotor field current. The rotor was found to be of salient pole construction and was determined to consist of a separate field and damper winding to allow for self-starting of the machine. The machine has an induction start mode but can be started in synchronous run mode due to the damper windings of the machine. In this mode of operation, the SM-100's starting torque is reduced as the rotor field winding is open-circuited and is unable to generate a magnetic field. The damper winding consists of a set of squirrel cage bars which are located on either side of the field winding coils in the rotor. The behavior and operating region of the SM-100 were also displayed through a V curve and generator capability curve.

7. CONCLUSIONS AND FUTURE WORK

In this thesis, the ITECH IT-M3633 power supply was used to conduct various experiments to model the Hampden SM-100 synchronous machines used in the Cal Poly Energy Conversion Laboratory. The classical modeling approaches for synchronous machines were used in conjunction with new experiments specifically developed for the SM-100 under test to develop both the classical model and a new model for performing analysis of the SM-100. The newly developed model for the SM-100 considers the machine's resistance and reactance parameters as a measurement of the stator windings, rotor damper windings, rotor field windings, and the machine core. This differs from the classical approach which contains only a single resistance and reactance component. From these experiments the stator to rotor turns ratio and rotor configuration were also determined to provide a more comprehensive model of the machine. A summary of the calculated parameters can be found in Table 10.

Table 10: Summary of Calculated Synchronous Machine Parameters

Test Case	Parameter	Value (Ω)
Direct Current Test	R_{stator}	4.3 Ω
Full Load Test	R_C	770.9 Ω
Rotor Applied DC Current	R_{field}	102 Ω
Rotor Parameter Measurement	R_{Damper}	135 Ω
Stator Reactance with Temperature Effect	X_S	26.2 Ω
Induction Machine Magnetizing Inductance	$X_{m\text{-}Induction}$	98.83 Ω
Stator to Rotor Field Winding Ratio	n	0.333
Stator to Rotor Mutual Inductance	$K_{S\text{-}F}$	$0.247\ \frac{V}{A*\frac{rad}{s}}$
Loaded Generator Test	$K_{R\text{-}S}$	$0.566\ \frac{V}{A*\frac{rad}{s}}$

While this thesis provided a better model for the SM-100 than what is possible with the classical approach, there are alternative experimental approaches that could further the model

proposed in this thesis. In the newly developed model, the magnetization reactance parameter was not given a value due to its variation with saturation, the loading on the machine, and the level of excitation current from the DC input. If these parameters could be considered and included in the model, the equivalent circuit model could provide a more comprehensive representation of the machine. As the SM-100 is a salient pole machine, the model could also be greatly improved by performing analysis in the direct-quadrature axis reference frame. As salient pole machines have non-uniform air gaps, this analysis could be used to model the variable reluctance of the SM-100. To incorporate these two factors, a future model for this project could be conducted in a direct-quadrature reference frame with a variable capacitance to account for changes in magnetizing reactance. To validate both the current model and any model developed in the future, simulations could also be conducted using the calculated parameters to better understand the results developed in this thesis. This would help to compare the traditional model to the newly developed model and identify any potential weaknesses of the new model. Many of the experiments in this thesis were also limited by the lack of angular position measurement system of the Cal Poly Energy Conversion Laboratory. A relationship between many of the synchronous machine parameters and the angular position of the rotor were identified in the experiments conducted for this thesis but were unable to be quantified and included as no angular position measurement device was available. If a device could be designed to incrementally change the position of the synchronous machines in the Cal Poly Energy Conversion Laboratory during locked rotor test conditions, many of the experiments conducted in this thesis could be better analyzed and quantified to improve the model for the SM-100 that has been developed in this thesis.

8. REFERENCES

[1] “Synchronous Motor,” JavaTpoint, [Online]. Available: https://www.javatpoint.com/synchronous-motor. [Accessed May 14, 2023].

[2] “Eddy Current Loss Formula,” Electricalvolt, [Online]. Available: https://www.electricalvolt.com/2019/08/eddy-current-loss-formula. [Accessed May 14, 2023].

[3] S. Zurek, “Magnetic saturation,” E-Magnetica, [Online]. Available: https://e-magnetica.pl/magnetic_saturation. [Accessed May 14, 2023].

[4] J. D. Santiago and J. G. de Oliveira, “Electric Machine Topologies in Energy Storage Systems,” in Energy Storage, R. I. Sheikh, Ed. Rijeka: IntechOpen, 2010.

[5] “Synchronous Motor Torque-Speed Characteristic Curve,” The Engineering Knowledge, [Online]. Available: https://www.theengineeringknowledge.com/synchronous-motor-torque-speed-characteristic-curve. [Accessed May 28, 2023].

[6] “Torque-Slip and Torque-Speed Characteristics of Induction Motor,” Electrical Technology, [Online]. Available: https://www.electricaltechnology.org/2022/04/torque-slip-torque-speed-characteristics-induction-motor.html. [Accessed May 28, 2023].

[7] ECE325-LabManual, The University of Tennessee, Knoxville, Tennessee, United States of America. [Online]. Available: http://web.eecs.utk.edu/~jsl/ECE325/ECE325-LabManual.pdf. [Accessed: May. 14, 2023].

[8] “M3600 Regenerative Power System from ITECH,” Itechate, [Online]. Available: https://www.itechate.com/en/product/dc-power-supply/IT-M3600.html. [Accessed May 14, 2023].

[9] “Synchronous Motor Starting Methods,” Electrical and Electronics Blog. [Online]. Available: https://howelectrical.com/synchronous-motor-starting-methods. [Accessed May 14, 2023].

[10] D. C. Aliprantis, B. T. Kuhn, S. D. Sudhoff, and T. J. Mccoy, “A Detailed Synchronous Machine Model,” SAE Technical Paper Series, Oct. 2002.

[11] P. Putta, “What is Generator Capability Curve?,” Electrical Engineering Materials – Experiences of a Power Engineer. [Online]. Available: https://electengmaterials.com/what-is-generator-capability-curve. [Accessed May 14, 2023].

APPENDICES

A SYNCHRONOUS MOTOR "V CURVE" DATA

Table 11: Synchronous Generator V Curve Experiment No Load Test Data

I_{DC} (A)	I_{AC} (A)	P (W)	Q (VAR)	S (VA)	PF
0.10	0.66	14.90	77.00	78.43	0.19
0.15	0.57	14.50	66.40	67.96	0.21
0.20	0.48	14.10	56.10	57.84	0.24
0.25	0.40	13.90	45.70	47.77	0.29
0.30	0.32	13.60	35.30	37.83	0.36
0.35	0.24	13.52	24.92	28.35	0.48
0.40	0.17	13.62	14.93	20.21	0.67
0.45	0.12	13.78	5.38	14.79	0.93
0.47	0.12	13.94	3.05	14.27	0.98
0.50	0.13	14.09	6.19	15.39	0.92
0.55	0.18	14.58	15.66	21.40	0.68
0.60	0.25	14.93	25.78	29.79	0.50
0.65	0.33	15.47	35.70	38.91	0.40
0.70	0.40	16.08	45.44	48.20	0.33
0.75	0.48	16.72	55.37	57.84	0.29
0.80	0.57	17.70	65.30	67.66	0.26
0.85	0.65	18.60	75.10	77.37	0.24
0.90	0.73	19.50	84.60	86.82	0.22
0.95	0.81	20.40	94.00	96.19	0.21
1.00	0.89	21.50	103.50	105.71	0.20

Table 12: Synchronous Generator V Curve Experiment Loaded Test Data

I_{DC} (A)	I_{AC} (A)	P (W)	Q (VAR)	S (VA)	PF
0.32	0.83	68.60	70.20	98.15	0.70
0.35	0.75	68.00	56.80	88.60	0.77
0.40	0.66	67.30	39.70	78.14	0.86
0.45	0.61	67.10	26.00	71.96	0.93
0.50	0.58	67.20	14.00	68.64	0.98
0.55	0.57	67.30	4.80	67.47	1.00
0.60	0.58	67.50	11.60	68.49	0.99
0.65	0.60	68.00	21.90	71.44	0.95
0.70	0.64	68.60	32.50	75.91	0.90
0.75	0.69	69.20	43.40	81.68	0.85
0.80	0.74	70.00	54.10	88.47	0.79
0.85	0.81	71.40	64.20	96.02	0.74
0.90	0.87	72.30	74.20	103.60	0.70
0.95	0.94	73.40	84.20	111.70	0.66
1.00	1.01	74.50	94.20	120.10	0.62

B SYNCHRONOUS MOTOR MECHANICAL LOSS TEST DATA

Table 13: Machine 1 Uncoupled No Load Test Data

Excitation Current (A)	Stator Voltage (V)	Stator Current (A)	Real Power (W)	Apparent Power (VA)	Reactive Power (VAR)	Power Factor	Phase Angle (°)	Lagging or Leading
0.4	119.9	0.1604	9.18	19.23	16.9	0.477	61.5	Lagging
0.5	119.9	0.0885	9.68	10.61	4.36	0.912	24.2	Leading
0.6	119.9	0.2166	10.38	25.98	23.81	0.4	66.4	Leading
0.7	119.9	0.3763	11.4	45.11	43.65	0.253	75.4	Leading
0.8	120	0.5401	12.87	64.79	63.5	0.199	78.5	Leading
0.9	119.8	0.701	14.6	84	82.7	0.173	80	Leading
1	119.9	0.859	16.5	103	101.7	0.16	80.8	Leading

Table 14: Coupled Machines No Load Test Data

Excitation Current (A)	Stator Voltage (V)	Stator Current (A)	Real Power (W)	Apparent Power (VA)	Reactive Power (VAR)	Power Factor	Phase Angle (°)	Lagging or Leading
0.4	119.9	0.1966	16.07	23.57	17.24	0.682	47	Lagging
0.5	119.9	0.1398	16.32	16.77	3.83	0.974	13.2	Leading
0.6	119.9	0.2422	17.08	29.05	23.5	0.588	54	Leading
0.7	119.9	0.3916	18.15	46.94	43.29	0.387	67.3	Leading
0.8	119.9	0.552	19.4	66.2	63.2	0.294	72.9	Leading
0.9	119.9	0.71	21.2	85.2	82.5	0.249	75.6	Leading
1	119.9	0.869	23.1	104.2	101.6	0.222	77.2	Leading

C STATOR TO ROTOR MUTUAL INDUCTANCE EXPERIMENT

Table 15: Synchronous Run Rotor Core Saturation Parameter Data

Vac (V)	Iac (A)	Vind @ Rotor (V)	Frequency of Vind @ Rotor (Hz)
0.79	0.0125	3.87	60.01
3.64	0.1311	12.59	60.01
7.43	0.2802	26.68	60
10.42	0.391	36.44	60.03
13.25	0.497	46.67	60.01
16.85	0.635	58.57	60.04
19.9	0.707	70	60.03
22.6	0.449	92.2	60.02
27.5	0.47	110.5	60.02
31.5	0.531	126	60.04
35.7	0.548	141	60.02

D OPEN CIRCUIT TEST DATA

Table 16: Open Circuit Test Data

I_{DC} (A)	V_{OC} (A)
0.01	5.26
0.05	21.14
0.1	43.2
0.15	66.2
0.2	88.2
0.25	110.4
0.3	132.4
0.35	154
0.4	175
0.45	194.5
0.486	207.7
0.5	212.2
0.55	227.3
0.6	239.1

E SHORT CIRCUIT TEST DATA

Table 17: Short Circuit Test Data

I_{DC} (A)	I_{AC} (A)
0.01	0.02
0.05	0.09
0.1	0.17
0.15	0.25
0.2	0.34
0.25	0.43
0.3	0.51
0.35	0.6
0.4	0.69
0.45	0.78
0.5	0.86
0.55	0.95
0.6	1.04
0.65	1.12
0.7	1.21
0.75	1.3
0.8	1.39
0.85	1.47
0.9	1.56
0.95	1.64
1	1.73

F LOADED GENERATOR TEST DATA

Table 18: Loaded Machine Test Data

I_{DC} (A)	V_{AN} (V)	I_A (A)
0.05	5.26	0.06
0.1	10.43	0.12
0.15	15.75	0.18
0.2	21.08	0.24
0.25	26.47	0.31
0.3	31.93	0.37
0.35	37.3	0.44
0.4	42.7	0.5
0.45	48.1	0.57
0.5	53.4	0.63
0.55	58.7	0.7
0.6	64.1	0.76
0.65	69.3	0.82
0.7	74.7	0.89
0.75	79.9	0.95
0.8	85.1	1.01
0.85	90.2	1.08
0.9	95.1	1.13
0.95	100.1	1.19
1	105	1.25

G GENERATOR CAPABILITY CURVE DATA

Table 19: 30mH Reactors in Series

I_{DC} Prime Mover	I_{DC} Generator	V_{AVG} (V)	I_{AVG} (A)	P_{TOTAL} (W)	S_{TOTAL} (VA)	Q_{TOTAL} (VAR)	PF
0.90	0.10	19.45	0.10	0.71	3.34	3.27	0.21
0.90	0.20	41.63	0.18	3.32	13.18	12.77	0.25
0.90	0.30	65.82	0.27	8.07	30.23	29.16	0.27
0.90	0.40	90.30	0.35	14.50	54.30	52.40	0.27
0.90	0.50	114.20	0.43	22.20	84.50	81.60	0.26
0.90	0.60	137.50	0.51	30.70	120.60	116.80	0.25
0.90	0.70	160.10	0.59	39.60	162.50	157.80	0.24
0.90	0.80	181.40	0.66	48.50	208.60	203.00	0.23
0.90	0.90	200.90	0.74	57.10	256.30	250.00	0.22

Table 20: 2 30mH Reactors in Series

I_{DC} Prime Mover	I_{DC} Generator	V_{AVG} (V)	I_{AVG} (A)	P_{TOTAL} (W)	S_{TOTAL} (VA)	Q_{TOTAL} (VAR)	PF
0.90	0.10	16.48	0.11	0.61	3.21	3.16	0.19
0.90	0.20	34.93	0.21	2.83	12.80	12.49	0.22
0.90	0.30	54.63	0.31	6.77	29.37	28.57	0.23
0.90	0.40	74.70	0.41	12.10	53.00	51.60	0.23
0.90	0.50	94.30	0.51	18.30	82.90	80.80	0.22
0.90	0.60	113.40	0.61	24.90	118.90	116.20	0.21
0.90	0.70	132.20	0.70	31.80	161.20	157.90	0.20
0.90	0.80	150.60	0.80	39.00	209.20	205.30	0.19
0.90	0.90	168.20	0.90	46.40	261.70	257.30	0.18

Table 21: 1 30mH Reactor

I_{DC} Prime Mover	I_{DC} Generator	V_{AVG} (V)	I_{AVG} (A)	P_{TOTAL} (W)	S_{TOTAL} (VA)	Q_{TOTAL} (VAR)	PF
0.90	0.10	10.96	0.13	0.41	2.51	2.46	0.16
0.90	0.20	23.21	0.26	1.87	10.38	10.15	0.18
0.90	0.30	35.97	0.39	4.41	24.00	23.43	0.18
0.90	0.40	48.84	0.51	7.73	43.44	42.47	0.18
0.90	0.50	61.23	0.64	11.30	67.90	66.50	0.17
0.90	0.60	73.40	0.77	15.10	97.70	95.90	0.15
0.90	0.70	85.50	0.90	19.20	132.70	130.40	0.14
0.90	0.80	97.50	1.03	23.60	173.40	170.60	0.14
0.90	0.90	109.30	1.16	28.30	218.60	215.20	0.13

Table 22: 2 35 Ω Resistors in Series

I_{DC} Prime Mover	I_{DC} Generator	V_{AVG} (V)	I_{AVG} (A)	P_{TOTAL} (W)	S_{TOTAL} (VA)	Q_{TOTAL} (VAR)	PF
0.90	0.10	28.44	0.08	3.68	4.11	2.00	0.90
0.90	0.20	61.49	0.17	17.27	18.03	5.53	0.96
0.90	0.30	96.50	0.26	41.80	42.90	10.20	0.97
0.90	0.40	131.40	0.34	76.30	77.70	16.10	0.98
0.90	0.50	164.50	0.42	118.20	120.00	23.10	0.99
0.90	0.60	194.90	0.49	164.60	166.70	31.40	0.99
0.90	0.70	221.30	0.56	210.40	213.20	40.40	0.99

Table 23: 1 35 Ω Resistor and 2 30mH Reactors in Series

I_{DC} Prime Mover	I_{DC} Generator	V_{AVG} (V)	I_{AVG} (A)	P_{TOTAL} (W)	S_{TOTAL} (VA)	Q_{TOTAL} (VAR)	PF
0.90	0.10	22.01	0.10	2.56	3.72	2.70	0.69
0.90	0.20	46.33	0.19	11.04	14.99	10.17	0.74
0.90	0.30	72.80	0.28	26.60	35.00	22.80	0.76
0.90	0.40	99.40	0.37	48.60	63.10	40.30	0.77
0.90	0.50	125.40	452.90	76.30	98.40	62.30	0.78
0.90	0.60	150.60	538.00	109.10	140.30	88.50	0.78
0.90	0.70	174.60	0.62	146.10	187.90	118.40	0.78
0.90	0.80	196.90	0.70	185.60	238.80	150.30	0.78
0.90	0.90	217.00	0.77	225.40	290.30	183.00	0.78

Table 24: 2 35 Ω Resistors and 2 30mH Reactors in Series

I_{DC} Prime Mover	I_{DC} Generator	V_{AVG} (V)	I_{AVG} (A)	P_{TOTAL} (W)	S_{TOTAL} (VA)	Q_{TOTAL} (VAR)	PF
0.90	0.10	26.65	0.08	2.84	3.74	2.46	0.76
0.90	0.20	57.31	0.16	13.03	15.52	8.55	0.84
0.90	0.30	89.70	0.23	31.10	35.90	18.40	0.87
0.90	0.40	122.40	0.30	56.60	64.40	21.20	0.88
0.90	0.50	153.60	0.37	87.80	99.30	46.90	0.88
0.90	0.60	183.00	0.44	123.10	139.00	65.30	0.89
0.90	0.70	209.20	0.50	159.80	180.60	84.60	0.88

Table 25: 1 35 Ω Resistor and 3 30mH Reactors in Series

I_{DC} Prime Mover	I_{DC} Generator	V_{AVG} (V)	I_{AVG} (A)	P_{TOTAL} (W)	S_{TOTAL} (VA)	Q_{TOTAL} (VAR)	PF
0.9	0.1	22.84	0.0905	2.1	3.58	2.93	0.586592179
0.9	0.2	48.74	0.1698	9.28	14.33	11.04	0.647592463
0.9	0.3	76.4	0.2474	22	32.7	24.5	0.672782875
0.9	0.4	104.6	0.3241	40.2	58.7	43.4	0.68483816
0.9	0.5	131.8	0.3981	62.5	90.9	66.9	0.687568757
0.9	0.6	158.1	0.4707	88.7	128.9	94.8	0.688130334
0.9	0.7	183.2	0.5413	118	171.8	126.6	0.686845169
0.9	0.8	205.6	0.607	147.7	216.2	159.8	0.683163737
0.9	0.9	224.9	0.665	176.2	259	192.3	0.68030888

Table 26: 2 35 Ω Resistor in Parallel in series with 3 30mH Reactors in Series

I_{DC} Prime Mover	I_{DC} Generator	V_{AVG} (V)	I_{AVG} (A)	P_{TOTAL} (W)	S_{TOTAL} (VA)	Q_{TOTAL} (VAR)	PF
0.9	0.1	20.15	0.0937	1.45	3.27	2.96	0.443425076
0.9	0.2	44.26	0.178	6.78	13.65	11.96	0.496703297
0.9	0.3	69.7	0.2595	16.2	31.3	27.1	0.517571885
0.9	0.4	95.5	0.3404	29.6	56.3	48.5	0.525754885
0.9	0.5	120.7	0.4186	46	87.5	75.2	0.525714286
0.9	0.6	145	0.4959	65.2	124.6	107.3	0.523274478
0.9	0.7	168.6	0.573	86.7	167.3	144.6	0.518230723
0.9	0.8	190.4	0.647	109.2	213.2	185	0.512195122
0.9	0.9	209.7	0.715	131.6	259.6	225.9	0.506933744

Table 27: 2 35 Ω Resistor in Parallel in series with 2 30mH Reactors in Series

I_{DC} Prime Mover	I_{DC} Generator	V_{AVG} (V)	I_{AVG} (A)	P_{TOTAL} (W)	S_{TOTAL} (VA)	Q_{TOTAL} (VAR)	PF
0.9	0.1	18.78	0.1059	1.86	3.45	2.93	0.539130435
0.9	0.2	39.55	0.2014	7.96	13.8	11.4	0.576811594
0.9	0.3	61.78	0.2974	18.94	31.82	25.9	0.59522313
0.9	0.4	84.4	0.393	34.6	57.4	46.4	0.602787456
0.9	0.5	106.4	0.4868	54.3	89.7	72.3	0.605351171
0.9	0.6	127.7	0.58	77.5	128.4	103.6	0.603582555
0.9	0.7	148.7	0.675	104.6	173.9	140.6	0.601495112
0.9	0.8	168.7	0.767	134.1	224.2	181.7	0.598126673
0.9	0.9	187.4	0.855	165.5	277.6	225.4	0.596181556

Table 28: 2 35 Ω Resistor in Parallel in series with 4 30mH Reactors in Series

I_{DC} Prime Mover	I_{DC} Generator	V_{AVG} (V)	I_{AVG} (A)	P_{TOTAL} (W)	S_{TOTAL} (VA)	Q_{TOTAL} (VAR)	PF
0.9	0.1	22.51	0.0893	1.41	3.48	3.21	0.405172414
0.9	0.2	48.25	0.1631	6.29	13.63	12.18	0.461482025
0.9	0.3	76	0.2351	14.9	30.9	27.3	0.482200647
0.9	0.4	104	0.3056	27	55	48.4	0.490909091
0.9	0.5	131.3	0.3735	41.7	84.9	74.7	0.491166078
0.9	0.6	157.7	0.4407	58.7	120.4	106.1	0.487541528
0.9	0.7	182.6	0.5058	77.1	160	141.4	0.481875
0.9	0.8	205.3	0.567	95.9	201.7	178.9	0.475458602
0.9	0.9	224	0.619	112.8	240	213.6	0.47

H HEAT EFFECT AND STATOR COIL REACTANCE CALCULATION DATA

Table 29: 0.9 A DC Excitation Synchronous Run Experiment Data Part 1

V_{DC} (V)	I_{DC} (A)	P_{DC} (W)	R_r	Heat factor	R_s	V_{LL} (V)	I_{AC} (A)	I_{AC}^2 (A^2)	$P_{3\text{-}Phase}$ (W)
97.63	0.90	87.87	108.5	1.06	4.56	207.00	0.75	0.567	74.0
98.93	0.90	89.04	109.9	1.07	4.62	207.00	0.76	0.582	90.0
100.10	0.90	90.09	111.2	1.09	4.68	207.00	0.77	0.598	101.0
100.25	0.90	90.23	111.4	1.09	4.68	207.10	0.79	0.624	123.0
100.64	0.90	90.58	111.8	1.09	4.70	207.20	0.81	0.656	146.0
101.01	0.90	90.91	112.2	1.10	4.72	207.20	0.83	0.689	167.0
101.19	0.90	91.07	112.42	1.10	4.73	207.10	0.84	0.707	177.50
101.36	0.90	91.22	112.6	1.10	4.73	207.00	0.85	0.726	188.00
101.80	0.90	91.62	113.1	1.11	4.75	207.10	0.88	0.771	210.0
102.11	0.90	91.90	113.5	1.11	4.77	206.90	0.91	0.821	232.0
102.39	0.90	92.15	113.8	1.11	4.78	207.00	0.94	0.878	256.0
102.76	0.90	92.48	114.2	1.12	4.80	207.10	0.97	0.933	278.0
103.05	0.90	92.75	114.5	1.12	4.81	207.00	1.00	1.000	301.0
103.30	0.90	92.97	114.8	1.12	4.82	206.90	1.04	1.071	322.0
103.60	0.90	93.24	115.1	1.13	4.84	207.10	1.07	1.143	343.0

Table 30: 0.9 A DC Excitation Synchronous Run Experiment Data Part 2

V_{DC} (V)	P_{mech} (W)	AC Efficiency	Dyno Friction (W)	$S_{3\text{-Phase}}$ (VA)	PF Leading	RPM	Torque (Lb-in)	$Q_{3\text{-Phase}}$ (VAR)	$Q_{1\text{-Phase}}$ (VAR)
97.63	4.7	6%	2.52	270.0	0.28	1800	0.22	-259.7	-86.6
98.93	10.4	12%	5.84	274.0	0.33	1800	0.49	-258.8	-86.3
100.10	21.2	21%	5.79	277.0	0.36	1800	1.00	-257.9	-86.0
100.25	42.7	35%	5.85	284.0	0.44	1800	2.01	-256.0	-85.3
100.64	64.6	44%	6.06	291.0	0.50	1800	3.04	-251.7	-83.9
101.01	85.6	51%	5.88	298.0	0.56	1800	4.03	-246.8	-82.3
101.19	95.26	54%	6.08	302.0	0.59	1800	4.49	-244.3	-81.4
101.36	104.9	56%	6.26	306.0	0.62	1800	4.94	-241.4	-80.5
101.80	126.6	60%	6.14	315.0	0.67	1800	5.96	-234.8	-78.3
102.11	146.6	63%	6.57	325.0	0.71	1800	6.90	-227.6	-75.9
102.39	172.5	67%	5.65	336.0	0.76	1800	8.12	-217.6	-72.5
102.76	192.6	69%	5.97	347.0	0.80	1800	9.07	-207.7	-69.2
103.05	215.6	72%	5.66	359.0	0.84	1800	10.15	-195.7	-65.2
103.30	237.0	74%	5.15	371.0	0.87	1800	11.16	-184.3	-61.4
103.60	258.1	75%	4.78	383.0	0.90	1800	12.15	-170.4	-56.8

Table 31: 0.9 A DC Excitation Synchronous Run Experiment Data Part 3

V_{DC} (V)	V_{core}	$X_{capacitive}$	$P_{DC} + P_{AC}$	AC&DC Efficiency	Sin (Theta)	Zs
97.63	115.7	-154.6	161.9	3%	-0.96	26.59
98.93	114.5	-151.9	179.0	6%	-0.94	26.60
100.10	113.6	-150.2	191.1	11%	-0.93	26.61
100.25	112.0	-147.1	213.2	20%	-0.90	26.62
100.64	110.4	-145.2	236.6	27%	-0.86	26.62
101.01	108.8	-143.8	257.9	33%	-0.83	26.62
101.19	107.9	-142.9	268.6	35%	-0.81	26.62
101.36	107.0	-142.3	279.2	38%	-0.79	26.62
101.80	105.4	-141.9	301.6	42%	-0.74	26.63
102.11	103.6	-141.5	323.9	45%	-0.70	26.63
102.39	101.8	-142.7	348.2	50%	-0.65	26.63
102.76	100.1	-144.8	370.5	52%	-0.60	26.64
103.05	98.2	-148.0	393.7	55%	-0.54	26.64
103.30	96.5	-151.5	415.0	57%	-0.49	26.64
103.60	94.9	-158.5	436.2	59%	-0.44	26.64

Table 32: Power Factor=1 Synchronous Run Experiment Data Part 1

V_{DC} (V)	I_{DC} (A)	P_{DC} (W)	R_r	Heat factor	R_s	V_{LL} (V)	I_{AC} (A)	I_{AC}^2 (A^2)	$P_{3\text{-}Phase}$ (W)
48.81	0.48	23.28	102.3	1.00	4.30	206.8	0.18	0.033	64.2
48.04	0.48	22.92	100.7	0.98	4.23	206.4	0.22	0.048	77.5
48.49	0.48	23.23	101.2	0.99	4.26	206.4	0.25	0.061	87.1
49.08	0.48	23.71	101.6	0.99	4.27	206.1	0.27	0.074	96.6
50.16	0.49	24.63	102.2	1.00	4.29	206.4	0.30	0.091	106.8
51.12	0.50	25.41	102.9	1.01	4.32	206.6	0.36	0.132	128.8
52.03	0.50	26.12	103.6	1.01	4.36	206.3	0.42	0.176	149.2
54.07	0.52	28.06	104.2	1.02	4.38	206.0	0.48	0.230	170.2
55.07	0.53	29.08	104.3	1.02	4.38	206.3	0.55	0.300	194.7
57.44	0.55	31.48	104.8	1.02	4.41	206.2	0.61	0.371	216.5
59.16	0.56	33.19	105.5	1.03	4.43	206.1	0.67	0.453	239.1
63.39	0.60	37.84	106.2	1.04	4.46	206.2	0.74	0.540	261.5
66.58	0.63	41.61	106.5	1.04	4.48	206.2	0.80	0.640	284.8
69.38	0.66	45.65	105.4	1.03	4.43	206.4	0.87	0.753	308.9
71.54	0.67	48.22	106.1	1.04	4.46	206.2	0.93	0.856	329.4

Table 33: Power Factor=1 Synchronous Run Experiment Data Part 2

V_{DC} (V)	P_{mech} (W)	AC Efficiency	Dyno Friction (W)	$S_{3\text{-Phase}}$ (VA)	PF Leading	RPM	Torque (Lb-in)	$Q_{3\text{-Phase}}$ (VAR)	$Q_{1\text{-Phase}}$ (VAR)
97.63	3.4	5%	2.12	65.2	0.99	1800	0.16	11.4	3.8
98.93	11.5	15%	3.81	78.4	0.99	1800	0.54	11.8	3.9
100.10	21.7	25%	3.55	88.3	0.99	1800	1.02	14.5	4.8
100.25	31.9	33%	3.26	97.1	1.00	1800	1.50	9.8	3.3
100.64	41.8	39%	3.26	107.7	1.00	1800	1.97	13.9	4.6
101.01	63.7	49%	3.12	129.9	0.99	1800	3.00	16.9	5.6
101.19	84.5	57%	2.79	150.1	0.99	1800	3.98	16.4	5.5
101.36	104.9	62%	2.75	171.0	1.00	1800	4.94	16.5	5.5
101.80	128.1	66%	2.89	195.7	1.00	1800	6.03	19.8	6.6
102.11	148.5	69%	3.04	217.7	1.00	1800	6.99	22.8	7.6
102.39	169.7	71%	3.12	240.4	1.00	1800	7.99	25.0	8.3
102.76	191.4	73%	2.96	262.5	1.00	1800	9.01	22.9	7.6
103.05	212.8	75%	3.13	285.7	1.00	1800	10.02	22.7	7.6
103.30	231.5	75%	4.46	310.3	1.00	1800	10.90	29.4	9.8
103.60	252.3	77%	3.87	330.5	1.00	1800	11.88	26.9	9.0

Table 34: Power Factor=1 Synchronous Run Experiment Data Part 3

V_{DC} (V)	V_{core}	X_m	AC & DC Efficiency	Sin (Delta)	$P_{3\text{-}Phase}$ Calculated	$P_{3\text{-}Phase}$ Percent Error	R_C
97.63	118.7	63.4	4%	0.04	65.2	1.47%	782.8
98.93	118.4	63.4	11%	0.05	78.4	1.10%	778.5
100.10	118.3	63.4	20%	0.05	88.2	1.28%	777.3
100.25	118.0	63.4	26%	0.06	97.1	0.48%	774.1
100.64	118.1	63.4	32%	0.07	107.7	0.85%	775.3
101.01	118.1	63.4	41%	0.08	129.8	0.79%	774.8
101.19	117.8	63.4	48%	0.09	150.1	0.61%	770.8
101.36	117.5	63.4	53%	0.11	171.0	0.48%	767.1
101.80	117.6	63.4	57%	0.12	195.8	0.57%	768.1
102.11	117.5	63.4	60%	0.14	217.5	0.46%	766.4
102.39	117.3	63.4	62%	0.15	240.3	0.48%	764.9
102.76	117.4	63.4	64%	0.16	262.5	0.39%	765.1
103.05	117.4	63.4	65%	0.18	285.7	0.32%	765.1
103.30	117.5	63.4	65%	0.19	310.3	0.46%	767.5
103.60	117.4	63.4	67%	0.21	330.4	0.29%	766.3

Table 35: Magnetizing Inductance Calculation Data Part 1

V_{LL} (V)	I_{AC}(A)	I_{AC}^2 (A^2)	$P_{3\text{-}Phase}$ (W)	P_{mech} (W)	AC Efficiency	Dyno Friction (W)	$S_{3\text{-}Phase}$ (VA)	PF lagging
206.50	0.83	0.684	66.9	4.1	6%	0.00	341.6	0.20

Table 36: Magnetizing Inductance Calculation Data Part 2

RPM	Torque (Lb-in)	$Q_{3\text{-}Phase}$ (VAR)	$Q_{1\text{-}Phase}$ (VAR)	Xs	V_{core}	X_m	P_{DC} + P_{AC}	AC&DC Efficiency
1780	0.19	340.97	113.66	26.2	84.9	63.43	66.9	6%